

# Influence of Linking Alkyl Chain Length on Photoinduced Intramolecular Electron Transfer in Bipyridine-Linked Porphyrin-RuO<sub>2</sub> Clusters

Ute Resch and Marye Anne Fox\*

Department of Chemistry, University of Texas at Austin, Austin, Texas 78712 (Received: December 27, 1990; In Final Form: March 26, 1991)

In a series of covalently linked *meso*-tris(octyloxyphenyl)porphyrin-RuO<sub>2</sub> composite clusters, the efficiency of photoinduced intramolecular electron transfer from the porphyrin to the covalently attached RuO<sub>2</sub> cluster depends on the length of the alkyl chain  $(-\text{CH}_2)_n$ ,  $n = 1, 4-7$  separating the surfactant-like porphyrin from the bipyridine ligating site. The broadening of the porphyrin Soret band and the observation of two distinct triplet-state lifetimes upon complexation to RuO<sub>2</sub> are best interpreted as arising from at least two distinct sets of conformers: (1) a family of folded conformers in which RuO<sub>2</sub> is complexed to the porphyrin  $\pi$ -electron system and (2) a family of more extended (noncomplexed) conformers. The complexed conformers exhibit broadened absorption spectra, decreased fluorescence quantum yields, and diminished triplet-state lifetimes compared to the noncomplexed conformers. Axial ligation of the zinc porphyrin to pyridine reduces intramolecular complexation between the porphyrin  $\pi$ -electron system and the RuO<sub>2</sub> cluster in ZnPB<sub>2</sub>R, resulting in unperturbed (narrow) absorption spectra, diminished fluorescence quenching, and a strong diminution of the relative amplitude of the short-lived porphyrin triplet state. However, even in pyridine, the fluorescence intensities, triplet yields, and singlet-state lifetimes of ZnPB<sub>2</sub>R are strongly decreased relative to the unbound porphyrin, whereas the porphyrin triplet-state lifetime is unaffected, suggesting intramolecular electron transfer as a major decay route of the porphyrin excited singlet state in the noncomplexed conformers.

## Introduction

Within the past few years, the investigation of parameters controlling electron transfer has been an area of intense research.<sup>1</sup> The dependence of electron-transfer rates on free energy and solvent has been studied in both bimolecular and covalently linked donor-acceptor systems.<sup>2-5</sup> Inter- and intramolecular electron transfer have been investigated as a function of the distance separating the donor and acceptor.<sup>6-10</sup> The distance dependence

of intermolecular electron-transfer has been determined in rigid media,<sup>6</sup> while intramolecular redox reactions have been studied in covalently attached donor-acceptor systems incorporating both rigid spacers<sup>7,8</sup> and flexible chains<sup>9,10</sup> as linkages. Rigid spacers provide the advantage of fixed distance and well-defined orientation between donor and acceptor,<sup>7,8</sup> whereas flexible linkages, which allow both the distance and the orientation to vary, may involve contributions from several conformers.<sup>9,10</sup> In such systems, the solvent may also influence the distribution of conformers and hence the electron-transfer rate.<sup>11</sup>

In flexible donor-acceptor systems, the role of the spacer in electronic coupling for intramolecular electron transfer has yet to be determined.<sup>12,13</sup> Electron transfer may take place either through-space (by direct interaction between donor and acceptor) or through-bond (along the flexible linking chain), with the relative importance of these two routes depending on the conformation of the donor-acceptor system.<sup>12,13</sup> In some covalently linked porphyrin-quinones, for example, the rates of both forward and back electron transfer appear to be affected by the ability of the donor and acceptor to assume one or more optimal conformations.<sup>9e,14</sup> Thus, for flexible donor-acceptor systems, dynamic conformational changes are important for defining the operative electron-transfer mechanism and hence their rates and efficiencies as components in artificial photosynthetic devices.<sup>11,15</sup>

(1) (a) Marcus, R. A.; Sutin, N. *Biochim. Biophys. Acta* **1985**, *811*, 265-282. (b) Closs, G. L.; Miller, J. R. *Science* **1988**, *240*, 440-447.

(2) (a) Rehm, D.; Weller, A. *Ber. Bunsen-Ges. Phys. Chem.* **1969**, *73*, 834-839. (b) Rehm, D.; Weller, A. *Isr. J. Chem.* **1970**, *8*, 259-271. (c) Greiner, G.; Pasquini, P.; Weiland, R.; Orthwein, H.; Rau, H. *J. Photochem. Photobiol., A: Chem.* **1990**, *51*, 179-915. (d) Ohno, T.; Yoshimura, A.; Mataga, N. *J. Phys. Chem.* **1990**, *94*, 4871-4876.

(3) Miller, J. R.; Beitz, J. V.; Huddleston, R. K. *J. Am. Chem. Soc.* **1984**, *106*, 5057-5068.

(4) (a) Miller, J. R.; Calcatera, L. T.; Closs, G. L. *J. Am. Chem. Soc.* **1984**, *106*, 3047-3049. (b) Wasielewski, M. R.; Niemczyk, M. P.; Svec, W. A.; Pewitt, E. P. *J. Am. Chem. Soc.* **1985**, *107*, 1080-1082. (c) Schmidt, J. A.; Siemiarczuk, A.; Weedon, A. C.; Bolton, J. R. *J. Am. Chem. Soc.* **1985**, *107*, 6112-6114. (d) Bolton, J. R.; Ho, T.-F.; Liauw, S.; Siemiarczuk, A.; Wan, C. S.; Weedon, A. C. *J. Chem. Soc., Chem. Commun.* **1985**, 559-560. (e) Irvine, M. P.; Harrison, R. J.; Beddard, G. S.; Leighon, P.; Sanders, J. K. M. *Chem. Phys.* **1986**, *104*, 315-324. (f) Oevering, H.; Paddon-Row, M. N.; Heppener, M.; Oliver, A. M.; Cotsaris, E.; Verhoeven, J. W.; Hush, N. S. *J. Am. Chem. Soc.* **1987**, *109*, 3258-3269. (g) Finckh, P.; Heitele, H.; Michel-Beyerle, M. E. *Chem. Phys.* **1989**, *138*, 1-10.

(5) (a) Miller, J. R. *Nouv. J. Chim.* **1987**, *11*, 83-89. (b) Joran, A. D.; Leland, B. A.; Felker, P. M.; Zewail, A. H.; Hopfield, J. J.; Dervan, P. B. *Nature* **1987**, *327*, 508-511.

(6) (a) Miller, J. R. *Science* **1975**, *189*, 221-222. (b) Miller, J. R.; Peeples, J. A.; Schmitt, M. J.; Closs, G. L. *J. Am. Chem. Soc.* **1982**, *104*, 6488-6493. (c) Strauch, S.; McLendon, G.; McGuire, M.; Guarr, T. J. *Phys. Chem.* **1983**, *87*, 3579-3581.

(7) Calcatera, L. T.; Closs, G. L.; Miller, J. R. *J. Am. Chem. Soc.* **1983**, *105*, 670-671. (b) Wasielewski, M. R.; Niemczyk, M. R. *J. Am. Chem. Soc.* **1984**, *106*, 5043-5045. (c) Joran, A. D.; Leland, B. A.; Geller, G. G.; Hopfield, J. J.; Dervan, P. B. *J. Am. Chem. Soc.* **1984**, *106*, 6090-6092. (d) Leland, B. A.; Joran, A. D.; Felker, P. M.; Hopfield, J. J.; Zewail, A. H.; Dervan, P. B. *J. Phys. Chem.* **1985**, *89*, 5571-5573. (e) Closs, G. L.; Calcatera, L. T.; Green, N. J.; Penfield, K. W.; Miller, J. R. *J. Phys. Chem.* **1986**, *90*, 3673-3683. (f) Verhoeven, J. W. *Pure Appl. Chem.* **1986**, *58*, 1285-1290. (g) Heiler, D.; McLendon, G.; Rogalski, P. J. *Am. Chem. Soc.* **1987**, *109*, 604-606. (h) Paddon-Row, M. N.; Oliver, A. M.; Warman, J. M.; Smit, J. K.; de Haas, M. P.; Oevering, H.; Verhoeven, J. W. *J. Phys. Chem.* **1988**, *92*, 6958-6962. (i) Johnson, M. D.; Miller, J. R.; Green, N. S.; Closs, G. L. *J. Phys. Chem.* **1989**, *93*, 1173-1176. (j) Sakata, Y.; Nakashima, S.; Goto, Y.; Tatsumi, H.; Misumi, S. *J. Am. Chem. Soc.* **1989**, *111*, 8979-8981.

(8) (a) Lindsey, J. S.; Mauzerall, D. C. *J. Am. Chem. Soc.* **1982**, *104*, 4498-4500. (b) Lindsey, J. S.; Mauzerall, D. C. *J. Am. Chem. Soc.* **1983**, *105*, 6528-6529.

(9) (a) Ho, T.-F.; McIntosh, A. R.; Bolton, J. R. *Nature* **1980**, *286*, 254-256. (b) Migita, M.; Okada, T.; Mataga, N.; Nishitani, S.; Kurata, N.; Sakata, Y.; Misumi, S. *Chem. Phys. Lett.* **1981**, *84*, 263-266. (c) Kong, J. L. Y.; Spears, K. G.; Loach, P. A. *Photochem. Photobiol.* **1982**, *35*, 545-553. (d) McIntosh, A. R.; Siemiarczuk, A.; Bolton, J. R.; Stillman, M. J.; Ho, T.-F.; Weedon, A. C. *J. Am. Chem. Soc.* **1983**, *105*, 7215-7223. (e) Siemiarczuk, A.; McIntosh, A. R.; Ho, T.-F.; Stillman, M. J.; Roach, K. J.; Weedon, A. C.; Bolton, J. R.; Connolly, J. S. *J. Am. Chem. Soc.* **1983**, *105*, 7224-7230. (f) Mataga, N.; Karen, A.; Okada, T.; Nishitani, S.; Kurata, N.; Sakata, Y.; Misumi, S. *J. Phys. Chem.* **1984**, *88*, 5138-5141.

(10) (a) Harriman, A.; Porter, G.; Wilowska, A. *J. Chem. Soc., Faraday Trans. 2*, **1984**, *80*, 191-204. (b) Harriman, A. *Inorg. Chim. Acta* **1984**, *88*, 213-216. (c) Kaji, N.; Aono, S.; Okura, I. *J. Mol. Catal.* **1986**, *36*, 201-203. (d) Nakamura, H.; Uehata, A.; Motonaga, A.; Ogata, T.; Matsuo, T. *Chem. Lett.* **1987**, 543-546. (e) Saito, T.; Hirata, Y.; Sato, H.; Yoshida, T.; Mataga, N. *Bull. Chem. Soc. Jpn.* **1988**, *61*, 1925-1931.

(11) Kanda, Y.; Sato, H.; Okada, T.; Mataga, N. *Chem. Phys. Lett.* **1986**, *129*, 306-309.

(12) Schmidt, J. A.; McIntosh, A. R.; Weedon, A. C.; Bolton, J. R.; Connolly, J. S.; Hurley, J. K.; Wasielewski, M. R. *J. Am. Chem. Soc.* **1988**, *110*, 1733-1740.

(13) Batteas, J. D.; Harriman, A.; Kanda, Y.; Mataga, N.; Nowak, A. K. *J. Am. Chem. Soc.* **1990**, *112*, 126-133.

(14) McIntosh, A. R.; Bolton, J. R.; Connolly, J. S.; Marsh, K. L.; Cook, D. R.; Ho, T.-F.; Weedon, A. C. *J. Phys. Chem.* **1986**, *90*, 5640-5646.

(15) Gnaedig, K.; Eisenthal, K. B. *Chem. Phys. Lett.* **1977**, *46*, 339-342.

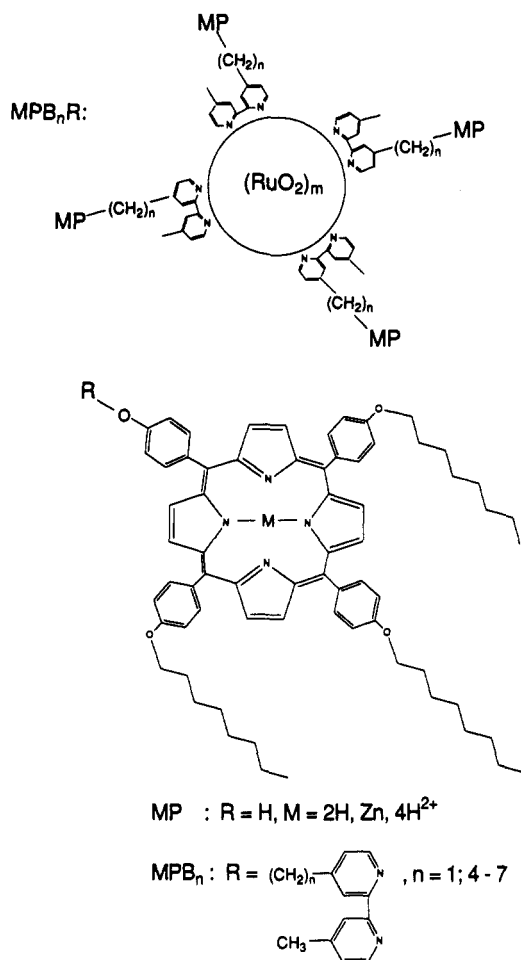


**Figure 1.** Schematic drawing of the bipyrindine-linked porphyrin-RuO<sub>2</sub> molecules MPB<sub>n</sub>R (M = 2H, Zn, 4H<sup>2+</sup>).

The synthesis and preliminary characterization of a surfactant-like *meso*-tris(octyloxyphenyl)porphyrin (MP with M = 2H, Zn, 4H<sup>2+</sup>), linked directly ( $n = 1$ ) to a derivative of 4,4'-dimethyl-2,2'-bipyridine (B), which is complexed to a RuO<sub>2</sub> cluster (R), MPBR (Figure 1), have been previously reported.<sup>16</sup> Recent photophysical studies of these systems suggest that the observed highly efficient quenching of the porphyrin fluorescence in ZnPBR is caused by electron transfer from the excited singlet state of the zinc porphyrin to the bound RuO<sub>2</sub>, whereas in the corresponding diacid derivative (M = 4H<sup>2+</sup>), the diminution of the porphyrin fluorescence may be ascribed to hole transfer.<sup>16,17</sup> In order to study the distance dependence of intramolecular photoinduced electron transfer from the porphyrin to the RuO<sub>2</sub> cluster, we synthesized analogous systems MPB<sub>n</sub>R (M = 2H, Zn, 4H<sup>2+</sup>), with the surfactantlike *meso*-tris(octyloxyphenyl)porphyrin and the bipyrindine ligating site separated by  $n$  methylene groups ( $n = 4-7$ ) (Figure 1). In these molecules, a one-electron photosensitizer (the porphyrin) is covalently attached, through a flexible chain of varying length, to a multielectron dark catalyst (RuO<sub>2</sub>) capable of both hydrogen and oxygen evolution.<sup>18,19</sup> MPB<sub>n</sub>R were designed for use in water-in-oil microemulsions, where the neutral water-insoluble porphyrin (M = 2H, Zn), in the organic phase

or at the interface, can transfer charge across the phase boundary to the hydrophilic RuO<sub>2</sub> catalyst in the aqueous phase.<sup>16,17</sup> In the microemulsions, the electrostatic field at the interface can assist the spatial separation of the radical ions produced in the primary electron transfer and can provide a barrier to back electron transfer.<sup>20</sup>

We report here the photophysical properties of the various MPB<sub>n</sub>R (Figure 1). We were particularly interested in determining the influence of the linking methylene chain length on the porphyrin singlet and triplet decay kinetics in different solvents. MPB<sub>n</sub>R (M = 2H, Zn, 4H<sup>2+</sup>) have been studied by fluorescence spectroscopy in homogeneous solution (THF, *p*-xylene-1-pentanol, pyridine) and in both anionic (sodium dodecyl sulfate, SDS) and cationic (dodecyltrimethylammonium bromide, DTAB) water-in-oil microemulsions. Flash photolysis experiments on a nanosecond and subnanosecond time scale have been carried out with the zinc derivatives (ZnPB<sub>n</sub>R) in different solvents.

## Experimental Section

**Materials.** Sodium dodecyl sulfate (SDS) and dodecyltrimethylammonium bromide (DTAB) were used as received from Aldrich and Kodak. All photochemical studies were carried out with Millipore water and spectroscopic grade solvents.

**Methods.** Nuclear magnetic resonance spectra (<sup>1</sup>H NMR and <sup>13</sup>C NMR) were obtained on a GE 500-MHz spectrometer. High-resolution mass spectra (EI) were measured on a VG Analytical mass spectrometer (ZAB2-E). Fast atom bombardment (FAB) mass spectra were performed on a Finnigan TSQ 70 instrument with the sample in a 3-nitrobenzyl alcohol matrix. Melting points were determined in a Mel-temp instrument and are uncorrected. Transmission electron micrographs (TEM) of the RuO<sub>2</sub> particles attached to the zinc porphyrin-bipyridine were recorded with a JEM 200 CX transmission electron microscope (JEOL). Absorption spectra were recorded on a Hewlett-Packard 8451A single beam spectrophotometer. Steady-state fluorescence spectra were measured on an SLM Aminco 500C spectrofluorometer. The fluorescence quantum yields of MPB<sub>n</sub>R ( $\Phi_f$ ) relative to those of the uncomplexed porphyrin, MPB<sub>n</sub> ( $\Phi_f^0$ ), were determined at matching optical densities ( $A = 0.08$ ). The fluorescence was excited at the maximum of the Soret bands of MPB<sub>n</sub> and MPB<sub>n</sub>R. All relative fluorescence quantum yields were calculated from integrated (albeit uncorrected) fluorescence spectra.

Time-resolved fluorescence measurements were performed via time-correlated single photon counting (SPC) using a mode-locked frequency-doubled Nd:YAG laser (Quantronix Model 416) synchronously pumping a cavity-dumped dye laser (Coherent Model 701-3D; Rhodamine 6G). The instrument response function was ca. 70 ps fwhm (full width at half-height of the maximum). The decay profiles were fit to a multiexponential decay function by using standard least-squares deconvolution techniques. The shortest lifetime which could be fit was 25 ps. The quality of the fits was evaluated by  $\chi^2$  test and by the randomness of the distribution of residuals. ZnP, ZnPB<sub>n</sub>, and ZnPB<sub>n</sub>R were excited at 586 nm; the emission was monitored at 610 nm. All measurements were carried out with air-saturated solutions.

For absorption measurements on a nanosecond time scale, excitation was provided by the second harmonic (532 nm, 11-ns pulse) from a Quantel YG481 Q-switched Nd:YAG laser. All flash photolysis experiments involving ZnP, ZnPB<sub>n</sub>, and ZnPB<sub>n</sub>R were carried out at a porphyrin concentration of  $3.3 \times 10^{-5}$  M ( $A_{532} = 0.115$ ) in a 1-cm cell. The triplet yields of ZnPB<sub>n</sub>R relative to ZnPB<sub>n</sub> were determined in Ar-saturated solutions at the same porphyrin concentration (matching absorption spectra). Each experiment was averaged over 50 shots. The triplet lifetimes of ZnP, ZnPB<sub>n</sub>, and ZnPB<sub>n</sub>R were measured at very low laser intensities in order to minimize triplet-triplet annihilation. The

(16) Gregg, B. A.; Fox, M. A.; Bard, A. J. *Tetrahedron* **1989**, *45*, 4707-4716.

(17) Resch, U.; Fox, M. A. *J. Phys. Chem.*, in press.

(18) (a) Kiwi, J. *J. Chem. Soc., Faraday Trans. 2*, **1982**, *78*, 339-345. (b) Christensen, P. A.; Harriman, A.; Porter, G. *J. Chem. Soc., Faraday Trans. 2* **1984**, *80*, 1451-1464. (c) Mills, A.; McMurray, N. *J. Chem. Soc., Faraday Trans. 1* **1988**, *84*, 379-390.

(19) (a) Amouyal, E.; Keller, P.; Moradpour, A. *J. Chem. Soc., Chem. Commun.* **1980**, 1019-1020. (b) Keller, P.; Moradpour, A.; Amouyal, E. *J. Chem. Soc., Faraday Trans. 1* **1982**, 3331-3340. (c) Amouyal, E.; Koffi, P. *J. Photochem.* **1985**, *29*, 227-242. (d) Kleijn, J. M.; Lyklema, *Colloid Polym. Sci.* **1987**, *265*, 1105-1113. (e) Kleijn, J. M.; Rouwendal, E.; Van Leeuwen, H. P.; Lyklema, J. *J. Photochem. Photobiol., A: Chem.* **1988**, *44*, 29-50.

(20) (a) Fendler, J. H. *Acc. Chem. Res.* **1976**, *9*, 153-161. (b) Graetzel, M. *Energy Resources through Photochemistry and Catalysis*; Academic: New York, 1983. (c) Mandler, D.; Degani, Y.; Willner, I. *J. Phys. Chem.* **1984**, *88*, 4366-4370.

measured triplet lifetimes may be oxygen limited and are thus regarded as apparent rather than true first-order lifetimes.<sup>21</sup>

Absorption measurements on a sub-nanosecond time scale were performed using a pulse-probe method as previously described.<sup>22</sup> The excitation source was a 30-ps pulse from a Quantel YG402 mode-locked Nd:YAG laser. After part of the laser fundamental (1064 nm) was converted to the second harmonic (532 nm) for sample excitation, the residual 1064-nm light was focused through a cell containing a continuum-generating medium (deuterated phosphoric acid in D<sub>2</sub>O) to produce a pulse of coherent white light with the same time profile as that of the laser pulse which was used as analyzing light. The probe and the excitation pulse were perpendicular to each other at the cuvette. Travelling through the cuvette were two 1-mm-diameter beams: one has passed through the first millimeter of excited sample; the other (reference beam) has passed through unexcited sample. Both beams were led to the entrance slit of an Instruments SA UFS200 spectrograph (200 lines/mm). The cathode of an image intensifier was positioned at the focal plane of the spectrograph. The detection array consisted of a proximity-focused image intensifier, two fiber optic conduits, and two linear 512 photodiode arrays (reticons) which were balanced before each experiment. Spectral resolution was determined as 0.6 nm per diode. The reticon output was passed via a Tracor Northern 6200 multichannel analyzer to a personal computer for storage, analysis, and display. The time profiles of the absorption spectra were acquired by repeatedly changing the path length of the analyzing beam. The available wavelength region was 450–750 nm, and the time window was 30 ps to 2.2 ns. The time resolution was limited by the width of the laser pulse (30 ps). All experiments involving ZnPB<sub>n</sub>R were carried out in a flow-through cell at an optical density of 1.0 at 532 nm. Flash photolysis studies of ZnP were carried out at an optical density of 0.35 at 532 nm.

**Microemulsions.** The anionic microemulsion consisted of *p*-xylene (56.7 wt%), 1-pentanol (20.1 wt %), water (12.4 wt %), and SDS (10.9 wt %). The cationic microemulsion contained *p*-xylene (54.7 wt %), 1-pentanol (19.9 wt %), water (12.3 wt %), and DTAB (13.2 wt %). The hydrodynamic radius of the water droplets was determined to 43 ± 3 Å for both microemulsions by light-scattering experiments.<sup>23</sup> The concentration of the water pools was calculated as 2.2 × 10<sup>-3</sup> M.<sup>23</sup>

**Synthesis.** The syntheses of each member of the series of the bromoalkyl bipyridines (B<sub>*n*</sub>, *n* = 4–7), the linked metalloporphyrin-bipyridines (MPB<sub>*n*</sub>), and the bipyridine-linked porphyrin-RuO<sub>2</sub> molecules (MPB<sub>*n*</sub>R) were conducted in parallel fashion. Details are given for the hexyl series here and spectral data for other members of the series (*n* = 4, 5, 7) are included in the Appendix. <sup>1</sup>H NMR and <sup>13</sup>C NMR spectra of B<sub>*n*</sub> were measured in CDCl<sub>3</sub> and those of ZnPB<sub>*n*</sub> in CDCl<sub>3</sub> containing 3.5% pyridine-*d*<sub>5</sub>.

**4-(6-Bromohexyl)-4'-methyl-2,2'-bipyridine (B<sub>6</sub>).** B<sub>6</sub> was prepared by the method of Ellison and Iwamoto<sup>24</sup> substituting the  $\alpha,\omega$ -dibromide for the  $\alpha$ -bromide. The crude product was chromatographed on silica (chloroform:ethyl acetate = 9:1). Recrystallization was accomplished from ethanol/water and yielded a white solid (45%). Mp: 70–72 °C. <sup>1</sup>H NMR (ppm):  $\delta$  1.34–1.38 (m, 2 H),  $\delta$  1.43–1.46 (m, 2 H),  $\delta$  1.67–1.71 (m, 2 H),  $\delta$  1.79–1.85 (m, 2 H),  $\delta$  2.41 (s, 3 H),  $\delta$  2.67 (t (*J* = 7.5 Hz), 2 H),  $\delta$  3.37 (t (*J* = 6.5 Hz), 2 H),  $\delta$  7.09–7.11 (m, 2 H),  $\delta$  8.19–8.20 (m, 2 H),  $\delta$  8.50–8.53 (m, 2 H). <sup>13</sup>C NMR (ppm):  $\delta$  21.2, 27.9, 28.3, 30.2, 32.6, 33.8, 35.3, 121.2, 122.0, 123.9, 124.6, 148.1, 148.9, 152.5, 156.0, 156.1. MS (EI), *m/e*: calcd for C<sub>17</sub>H<sub>21</sub>N<sub>2</sub><sup>79</sup>Br, 332.0914; found 332.0888.

**ZnPB<sub>6</sub>.** 4-(6-Bromohexyl)-4'-methyl-2,2'-bipyridine (B<sub>6</sub>) was linked to 5,10,15-tris(4-octyloxyphenyl)-20-(4-hydroxyphenyl)-

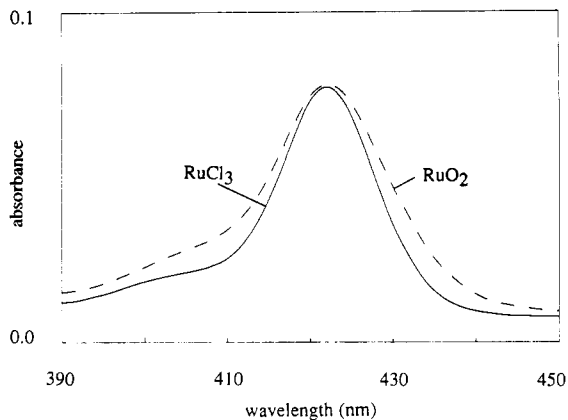


Figure 2. Absorption spectra (Soret region) of H<sub>2</sub>PB<sub>6</sub>, complexed to RuCl<sub>3</sub> (—) and RuO<sub>2</sub> (---); *c*<sub>Ru</sub>/*c*<sub>P</sub> = 3:1. The RuCl<sub>3</sub>-coordinated species shows the same absorption spectrum (Soret region) as the uncomplexed porphyrin H<sub>2</sub>PB<sub>6</sub>.

porphyrin (H<sub>2</sub>P), yielding H<sub>2</sub>PB<sub>6</sub>, as previously described.<sup>16</sup> The zinc derivative, ZnPB<sub>6</sub>, was obtained by metallation of H<sub>2</sub>PB<sub>6</sub> with Zn(OAc)<sub>2</sub> in THF and purified by column chromatography on silica gel in the dark (eluent CHCl<sub>3</sub>, addition of ethyl acetate) and recrystallized from CHCl<sub>3</sub>/CH<sub>3</sub>OH. Yield: 65% of a purple solid; mp 160–163 °C. <sup>1</sup>H NMR (ppm):  $\delta$  0.93 (t (*J* = 7.0 Hz), 9 H),  $\delta$  1.34–1.46 (m, 24 H),  $\delta$  1.52–1.54 (m, 2 H),  $\delta$  1.59–1.62 (m, 8 H),  $\delta$  1.80–1.82 (m, 2 H),  $\delta$  1.94–1.97 (m, 8 H),  $\delta$  2.39 (s, 3 H),  $\delta$  2.76 (t (*J* = 7.5 Hz), 2 H),  $\delta$  4.21 (t (*J* = 6.5 Hz), 8 H),  $\delta$  7.20–7.30 (m, 10 H),  $\delta$  8.07–8.09 (m, 8 H),  $\delta$  8.33–8.41 (m, 2 H),  $\delta$  8.52–8.61 (m, 2 H),  $\delta$  8.90–8.91 (m, 8 H). <sup>13</sup>C NMR (ppm):<sup>25</sup>  $\delta$  13.9, 20.9, 22.5, 25.8, 26.0, 29.1, 29.1, 29.3, 29.3, 29.5, 30.1, 31.6, 35.2, 67.8, 68.0, 112.0, 119.9, 120.8, 121.5, 122.7, 122.9, 123.0, 123.1, 123.4, 125.0, 131.0, 131.1, 131.2, 135.0, 135.2, 135.2, 135.3, 135.35, 148.7, 148.8, 149.0, 149.1, 149.2, 149.9, 150.1, 158.3. MS (FAB), *m/e*: calcd for C<sub>85</sub>H<sub>96</sub>O<sub>4</sub>N<sub>6</sub>Zn, 1329; found 1329.

**ZnPB<sub>6</sub>R.** A synthesis and characterization parallel to that employed in the synthesis of H<sub>2</sub>PB<sub>*n*</sub>R and ZnPB<sub>*n*</sub>R, *n* = 1 was employed.<sup>16,17</sup> H<sub>2</sub>PB<sub>6</sub> (1 × 10<sup>-4</sup> M) and RuCl<sub>3</sub> (ruthenium-to-porphyrin molar ratio, *c*<sub>Ru</sub>/*c*<sub>P</sub> = 1:3) were heated under reflux for 25 min in a mixture of dry THF/methanol (50 mL/10 mL). Basic hydrolysis of the porphyrin-bipyridine coordinated RuCl<sub>3</sub> complex in the presence of excess RuCl<sub>3</sub> yielded porphyrin-bipyridine capped RuO<sub>2</sub> particles, H<sub>2</sub>PB<sub>6</sub>R.<sup>16,17,26</sup> Unlike H<sub>2</sub>PBR (*n* = 1), no cleavage of the ether bond producing free porphyrin, H<sub>2</sub>P, was observed for H<sub>2</sub>PB<sub>6</sub>R.<sup>17</sup> ZnPB<sub>6</sub>R, obtained by metallation of H<sub>2</sub>PB<sub>6</sub>R, was purified by column chromatography on cellulose (eluent CHCl<sub>3</sub>, addition of CH<sub>3</sub>OH and CH<sub>3</sub>CN) in the dark and was recrystallized from CHCl<sub>3</sub>/CH<sub>3</sub>OH. H<sub>2</sub>PB<sub>6</sub>R and ZnPB<sub>6</sub>R are purple redispersible powders which readily dissolve in THF, chlorinated solvents, pyridine, and *p*-xylene/1-pentanol and in the microemulsions.<sup>17</sup> The diacid derivative, H<sub>4</sub><sup>2+</sup>PB<sub>6</sub>R, obtained by treating the corresponding free base or zinc species with a strong acid (HCl or trifluoroacetic acid), was characterized by absorption and fluorescence spectroscopy.<sup>16,17</sup>

## Results and Discussion

**Dependence of the Absorption Spectra of MPB<sub>*n*</sub>R (M = 2 H, Zn, 4 H<sup>2+</sup>) on Spacer Chain Length.** Coordination to RuCl<sub>3</sub> does not affect the absorption spectra of H<sub>2</sub>PB<sub>*n*</sub>. However, conversion of the H<sub>2</sub>PB<sub>*n*</sub>-coordinated RuCl<sub>3</sub> in the presence of excess (unbound) RuCl<sub>3</sub> (porphyrin-to-ruthenium molar ratio, *c*<sub>Ru</sub>/*c*<sub>P</sub> = 3:1) to a coordinated RuO<sub>2</sub> cluster, H<sub>2</sub>PB<sub>*n*</sub>R,<sup>16,17,26</sup> respectively, results in a slight broadening of the porphyrin Soret band (Figure 2). The Soret bandwidth depends on the ruthenium-to-porphyrin molar ratio (*c*<sub>Ru</sub>/*c*<sub>P</sub>) when bound to a RuO<sub>2</sub> cluster: at *c*<sub>Ru</sub>/*c*<sub>P</sub>

(21) Linschitz, H.; Steel, C.; Bell, J. A. *J. Phys. Chem.* **1962**, *66*, 2574–2576.

(22) Atherton, S. J.; Hubig, S. M.; Callan, T. J.; Duncanson, J. A.; Snowden, P. T.; Rodgers, M. A. *J. Phys. Chem.* **1987**, *91*, 3137–3140.

(23) Resch, U.; Fox, M. A. *Am. Chem. Soc. Symp. Ser.*, in press.

(24) Ellison, D. K.; Iwamoto, R. T. *Tetrahedron Lett.* **1983**, *45*, 4707–4716.

(25) The very similar chemical shifts of many of the <sup>13</sup>C resonances made resolution of overlapping peaks impossible in some cases.

(26) Blondeel, G.; Harriman, A.; Porter, G.; Urwin, D.; Kiwi, J. *J. Phys. Chem.* **1983**, *87*, 2629–2636.

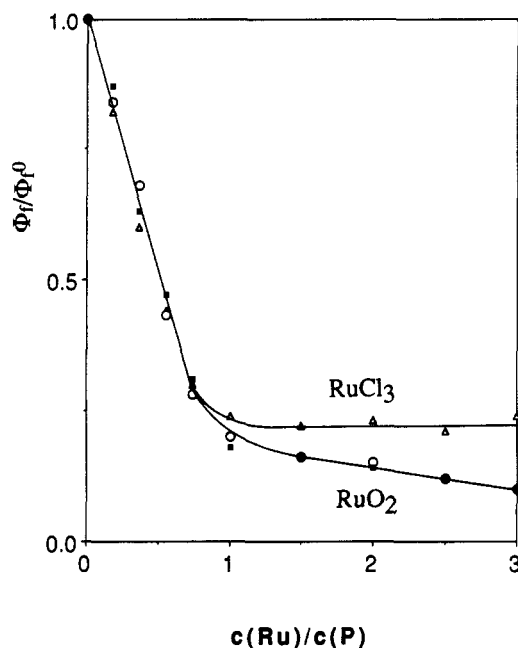


**Figure 3.** Relative fluorescence quantum yield ( $\Phi_f/\Phi_f^0$ ) of  $H_2PB_5$  in THF as a function of the molar ratio of ruthenium to porphyrin ( $c_{Ru}/c_P$ ):  $\Delta$ ,  $RuCl_3$ ;  $\circ$ ,  $RuO_2$ ;  $\blacksquare$ ,  $RuO_2$  (hydrolysis under dilute conditions; dilution by a factor of 100).

$< 1$ , the Soret band is not affected, whereas at  $c_{Ru}/c_P > 1$  the Soret band broadens with increasing ruthenium concentration, i.e., with increasing cluster size. This spectral broadening is not merely caused by intermolecular porphyrin aggregation during the generation of the  $RuO_2$  cluster since for  $H_2PB_nR$  ( $c_{Ru}/c_P = 3:1$ ), conversion of the complexed  $RuCl_3$  to a  $RuO_2$  cluster at different porphyrin ( $c_P = 1 \times 10^{-4}$  and  $1 \times 10^{-6}$  M) and ruthenium ( $c_{Ru}/c_P = 3:1$ ) concentrations leads to the same changes in the absorption spectra and fluorescence quenching (see below, Figure 3). For  $H_2PB_nR$  and  $H_4^{2+}PB_nR$  (which were obtained by protonation of the free base porphyrins), the magnitude of the Soret broadening upon  $RuO_2$  generation depends on the length of the methylene chain separating the porphyrin from the  $RuO_2$  cluster (Table I). For  $n = 4-6$ , the Soret bands of  $H_2PB_nR$  (full width at half-height of the maximum absorption of the Soret band (fwhm) = 16 nm) and  $H_4^{2+}PB_nR$  (fwhm = 20 nm) are broader than those of  $H_2PB_n$  (fwhm = 13 nm) and  $H_4^{2+}PB_n$  (fwhm = 16 nm). In contrast, the absorption spectra of  $H_2PB_nR$  and  $H_4^{2+}PB_nR$  ( $n = 1$  or 7) show nearly no broadening. A similar chain length dependent Soret broadening is also observed for  $ZnPB_nR$  in THF, *p*-xylene/1-pentanol and in the microemulsions (Table I). However, for  $H_2PB_nR$ ,  $ZnPB_nR$ , and  $H_4^{2+}PB_nR$ , no red shift of the Soret bands or changes in the shapes or positions of the Q bands could be detected.

Intermolecular and intramolecular porphyrin aggregation in the redispersible  $MPB_nR$  can be ruled out as an explanation for the observed Soret broadening since the absorption spectra of redissolved  $MPB_nR$  remain unchanged over a wide concentration range ( $4 \times 10^{-8}$  to  $2 \times 10^{-4}$  M) and since the absorption maxima of  $MPB_nR$  are not shifted relative to  $MPB_n$ , whereas dimerization of porphyrins either results in a splitting<sup>27</sup> or a blue shift<sup>28</sup> of the Soret band depending on the orientation of the porphyrin molecules. However, similar perturbations of the absorption spectra have been reported for a series of *meso*-tetratolylporphyrins covalently attached to various quinones via flexible diamide linkages with the two amides being separated by  $n$  methylene groups ( $n = 2, 3$ , and 4).<sup>9e</sup> In these porphyrin-quinones, the broadened absorption spectra are assigned to perturbed (complexed) conformers in which folding of the quinone over the  $\pi$ -system of the porphyrin leads to direct electronic interaction between the two

**TABLE I:** Soret Bandwidth (fwhm), Relative Fluorescence Quantum Yields of  $MPB_n$  Coordinated to either  $RuCl_3$  or  $RuO_2$  ( $MPB_nR$ ), and Calculated Intramolecular Electron-Transfer Rate Constants ( $k_{et}$ ) in Tetrahydrofuran

M	n	$RuCl_3^a$		$RuO_2^a$		
		fwhm, <sup>b</sup> nm	$\Phi_f/\Phi_f^{0c,d}$	fwhm, <sup>b</sup> nm	$\Phi_f/\Phi_f^{0c,e}$	$k_{et}^{e,f} \times 10^{-9}$ , s <sup>-1</sup>
2 H	1	13	0.05	14	0.05	1.9
2 H	4	13	0.20	17	0.07	1.3
2 H	5	13	0.25	17	0.11	0.79
2 H	6	13	0.30	16	0.15	0.56
2 H	7	13	0.35	14	0.30	0.23
Zn	1		g	13 <sup>h</sup>	0.03	23
Zn	4		g	16 <sup>h</sup>	0.06	11
Zn	5		g	16 <sup>h</sup>	0.09	7.2
Zn	6		g	15 <sup>h</sup>	0.14	4.4
Zn	7		g	13 <sup>h</sup>	0.27	1.9
4 H <sup>2+</sup>	1	16	0.09	17	0.09	4.8
4 H <sup>2+</sup>	4	16	0.29	20	0.17	2.3
4 H <sup>2+</sup>	5	16	0.37	20	0.23	1.6
4 H <sup>2+</sup>	6	16	0.42	19	0.30	1.1
4 H <sup>2+</sup>	7	16	0.48	17	0.44	0.61

<sup>a</sup>Porphyrin-to-ruthenium ratio,  $c_{Ru}/c_P = 1:3$ . <sup>b</sup>Full width at half-height of the maximum absorption of the Soret band: fwhm( $H_2PB_n$ ) = 13 nm; fwhm( $ZnPB_n$ ) = 11 nm; fwhm( $H_4^{2+}PB_n$ ) = 16 nm, all independent of solvent. <sup>c</sup>Fluorescence quantum yield of ruthenium-coordinated  $MPB_n$  ( $\Phi_f$ ) relative to the fluorescence quantum yield of uncomplexed  $MPB_n$  ( $\Phi_f^0$ ). <sup>d</sup>Complexed to  $RuCl_3$ . <sup>e</sup>Complexed to  $RuO_2$ . <sup>f</sup> $k_{et}$  was calculated from eq. 1, assuming a single conformation. <sup>g</sup>The reaction of  $ZnPB$  with  $RuCl_3$  leads to partial protonation of the zinc porphyrin. <sup>h</sup>For  $ZnPB_nR$ , identical fwhm are observed in THF, *p*-xylene/1-pentanol, and in the microemulsions.

chromophores, i.e., to the formation of intramolecular complexes. More extended porphyrin-quinone conformers do not exhibit spectral perturbations.<sup>9e</sup>

The broadened Soret bands of  $MPB_nR$  are thus also interpreted as arising from contributions of complexed conformers in which folding of the  $RuO_2$  cluster at the end of the methylene-bipyridine chain over the porphyrin macrocycle leads to intramolecular complexation between the  $\pi$ -electron system of the porphyrin and the  $RuO_2$ . The more extended (noncomplexed)  $MPB_nR$  conformers presumably do not show spectral broadening. The extent of this intramolecular complexation in  $MPB_nR$  depends on the methylene chain length as indicated by the chain length dependent Soret broadening: for  $n = 4-6$ , complexation appears to be more significant than for  $n = 7$ . For  $n = 1$ , presumably no folding occurs. This interpretation is consistent with fluorescence measurements and triplet decay kinetics of  $MPB_nR$  discussed below, and a similar dependence of the Soret broadening on linking chain length has also been reported for the porphyrin-quinones.<sup>9e</sup>

**Dependence of the Fluorescence Spectra and the Relative Fluorescence Quantum Yields of  $MPB_nR$  on Spacer Length.** Complexation of  $MPB_n$  ( $M = 2H, 4H^{2+}$ ) to  $RuCl_3$  leads to a strong decrease in the porphyrin fluorescence, the magnitude of which depends on the spacer length,  $n$ , between the porphyrin (MP) and the bipyridine ligating site (B) (Table I). Upon conversion of the  $MPB_n$ -coordinated  $RuCl_3$  to  $MPB_nR$  ( $n = 4-7$ ),<sup>16,17,26</sup> a further decrease of the fluorescence intensity is observed (Table I) with this effect being much less pronounced for  $n = 7$ . For  $n = 1$ , the  $RuCl_3$ -coordinated MPB and MPBR exhibit the same relative fluorescence quantum yield.<sup>17</sup> The extent of fluorescence quenching in the free base porphyrin,  $H_2PB_nR$ , is very similar to that in the zinc derivatives,  $ZnPB_nR$ , whereas for the corresponding diacid porphyrin species,  $H_4^{2+}PB_nR$ , less efficient fluorescence quenching is observed (Table I).

For  $H_2PB_5$ , the relative fluorescence quantum yields ( $\Phi_f/\Phi_f^0$ ) of both the  $RuCl_3$ - and the  $RuO_2$ -coordinated species were determined as a function of the molar ruthenium-to-porphyrin ratio ( $c_{Ru}/c_P$ ) in THF (Figure 3) analogous to the previously described absorption measurements. For  $c_{Ru}/c_P < 1$ , the porphyrin fluorescence is equally quenched by coordination to either  $RuCl_3$  or  $RuO_2$ , the linear decrease of the porphyrin fluorescence with increasing ruthenium concentration indicating that the fluorescence

(27) Kasha, M.; Rawls, H. R.; Ashraf el-Bayoumi, M. *Pure Appl. Chem.* **1965**, *11*, 371-393.

(28) Brochette, P.; Pileni, M. P. *Nouv. J. Chim.* **1985**, *9*, 551-554.

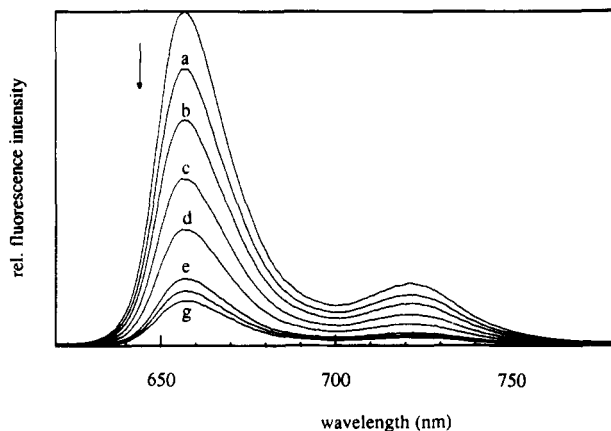


**Figure 4.** Uncorrected fluorescence spectra of H<sub>2</sub>PB<sub>5</sub>, after complexation with various amounts of RuO<sub>2</sub>;  $c_{\text{Ru}}/c_{\text{P}} = 0.18$  (a), 0.37 (b), 0.55 (c), 0.74 (d), 1.00 (e), 2.00 (f), and 3.00 (g); excitation was at 422 nm; solvent, THF.

is quenched by bound ruthenium. However, at  $c_{\text{Ru}}/c_{\text{P}} > 1$ , the relative fluorescence quantum yield reaches a plateau for RuCl<sub>3</sub> (at  $c_{\text{Ru}}/c_{\text{P}} > 1$ , the solution contains a mixture of RuCl<sub>3</sub> coordinated to MPB<sub>n</sub> and unbound RuCl<sub>3</sub> since every MPB<sub>n</sub> can complex only one RuCl<sub>3</sub> molecule), but decreases slightly with increasing ruthenium concentration for RuO<sub>2</sub>. For MPB<sub>5</sub>R, generation of the RuO<sub>2</sub> cluster in the presence of excess (unbound) RuCl<sub>3</sub> at  $c_{\text{P}}/c_{\text{Ru}} > 1$  results in the formation of bigger RuO<sub>2</sub> clusters; i.e., more than one RuO<sub>2</sub> is attached to a porphyrin.<sup>16</sup> For H<sub>2</sub>PB<sub>n</sub>R, the Soret broadening (which is attributed to intramolecular complexation) and the reduction in the relative fluorescence quantum yield upon RuO<sub>2</sub> formation similarly depend on the ruthenium-to-porphyrin molar ratio, suggesting that intramolecular complexation between the porphyrin and RuO<sub>2</sub> via a folded conformation also accounts for the observed further decrease in porphyrin fluorescence intensity. Size-dependent changes in the redox potentials of the RuO<sub>2</sub> cluster<sup>29,30</sup> cannot cause this effect since TEM pictures of ZnPB<sub>n</sub>R and ZnPB<sub>5</sub>R indicate the formation of RuO<sub>2</sub> clusters of similar sizes, i.e., that surface capping is controlled by the size of the ligating group, not by its proximity to the porphyrin sensitizer.

Interestingly, the fluorescence spectra of H<sub>2</sub>PB<sub>n</sub>R, ZnPB<sub>n</sub>R, and H<sub>4</sub><sup>2+</sup>PB<sub>n</sub>R show neither noticeable broadening nor spectral shifts (Figures 4 and 5), unlike reports of broadening and a red shift of the fluorescence maxima of the linked porphyrin-quinones, especially when excited in the region of the absorption broadening.<sup>9c</sup> For example, the fluorescence spectra of ZnPB<sub>n</sub> and ZnPB<sub>n</sub>R (Figure 5) are independent of the excitation wavelength in the broadened Soret region (415, 430, and 440 nm, inset of Figure 5). ZnPB<sub>n</sub> and ZnPB<sub>n</sub>R also show identical excitation spectra.

In the porphyrin-quinones, perturbed fluorescence spectra are ascribed to contributions from complexed conformers where enhanced radiationless decay from the porphyrin excited state leads to some fluorescence quenching.<sup>9c</sup> However, in both complexed and extended porphyrin-quinone conformers, electron transfer from the excited porphyrin singlet state to the quinone has been reported, with conformational heterogeneity resulting in a distribution of electron transfer rates.<sup>9d,e,14</sup> The unperturbed fluorescence spectra of MPB<sub>n</sub>R suggest that the complexed conformers exhibit nearly complete fluorescence quenching, presumably caused by enhanced spin-orbit coupling (see triplet decay kinetics below), so that the observed fluorescence derives virtually entirely from the more extended (noncomplexed) conformers.

(29) (a) Rossetti, R.; Nakahara, S.; Brus, L. E. *J. Chem. Phys.* **1983**, *79*, 1086-1988. (b) Brus, L. E. *J. Chem. Phys.* **1983**, *79*, 5566-5571. (c) Brus, L. E. *J. Phys. Chem.* **1986**, *90*, 2555-2560. (d) Henglein, A. *Chem. Rev.* **1989**, *89*, 1861-1873.

(30) Henglein, A.; Tausch-Treml, R. *J. Colloid Interface Sci.* **1981**, *80*, 84-93.

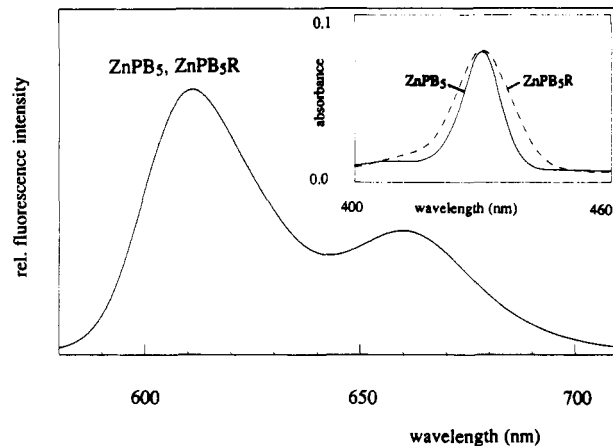


**Figure 5.** Superposition of normalized uncorrected fluorescence spectra of ZnPB<sub>5</sub> and ZnPB<sub>5</sub>R in *p*-xylene/1-pentanol, obtained by excitation at 415, 430, and 440 nm; the same fluorescence spectra for ZnPB<sub>5</sub> and ZnPB<sub>5</sub>R are observed independent of excitation wavelength. Inset: absorption spectra (Soret region) of ZnPB<sub>5</sub> and ZnPB<sub>5</sub>R in *p*-xylene/1-pentanol.

**Calculated Electron-Transfer Rates for MPB<sub>n</sub>R.** For MPBR ( $n = 1$ ), fluorescence quenching is presumably caused by electron transfer from the porphyrin singlet excited state rather than by either energy transfer or by spin-orbit coupling due to the heavy atom effect of ruthenium.<sup>16,17</sup> Thus, if we assume conformational homogeneity,<sup>31</sup> we can estimate the rate constants for electron transfer in the bipyridine-linked porphyrin-RuO<sub>2</sub> molecules, MPB<sub>n</sub>R, from the relative fluorescence quantum yields ( $\Phi_f/\Phi_f^0$ ) of MPB<sub>n</sub>R and the experimental singlet-state lifetimes ( $\tau_f^0$ ) of the uncomplexed porphyrins, MPB<sub>n</sub>, in THF ( $\tau_f^0(\text{H}_2\text{PB}_n) = 10.2$  ns,  $\tau_f^0(\text{ZnPB}_n) = 1.4$  ns, and  $\tau_f^0(\text{H}_4^{2+}\text{PB}_n) = 2.1$  ns):

$$k_{\text{et}} = (\Phi_f^0/\Phi_f - 1)/\tau_f^0 \quad (1)$$

The relative fluorescence quantum yields of MPB<sub>n</sub>R and, thus, the rate constants for electron transfer depend on the spacer length,  $n$ , separating the porphyrin and the bipyridine with slower electron transfer being observed as the length of the chain increases (Table I). The slower electron-transfer rates for H<sub>2</sub>PB<sub>n</sub>R than for ZnPB<sub>n</sub>R may be attributed to differences in the excited-state redox potentials.<sup>4b,16</sup> The excited singlet state of a zinc tetraphenylporphyrin is a strong reducing agent with an excited-state oxidation potential of ca. -1.4 V vs SCE.<sup>16,32,33</sup> The excited singlet state of the free base derivative is a weaker reductant (excited-state oxidation potential ca. -1.0 V vs SCE), but a slightly stronger oxidant (excited-state reduction potential ca. 0.7 V vs SCE) than the zinc porphyrin (excited-state reduction potential ca. 0.6 V vs SCE).<sup>16,32,33</sup>

For H<sub>4</sub><sup>2+</sup>PB<sub>n</sub>R, hole transfer from the excited porphyrin to the RuO<sub>2</sub> moiety may be assumed since the excited singlet state of the diacid porphyrin should be a strong oxidant (excited-state reduction potential ca. 1.5 V vs SCE, estimated from the diacid form of octaethylporphyrin, H<sub>4</sub><sup>2+</sup>OEP).<sup>16,33</sup>

**Dependence of Triplet Decay Kinetics of ZnPB<sub>n</sub>R on Spacer Length. A. Triplet Yield.** Spectroscopic studies (nanosecond-time-resolved absorption spectroscopy) of the triplet states of ZnPB<sub>n</sub>R in *p*-xylene/1-pentanol and in the microemulsions show that complexation of ZnPB<sub>n</sub> to RuO<sub>2</sub> also leads to a strong decrease in the porphyrin triplet yield. However, because of the substantial amount of fast decaying porphyrin triplet (see triplet lifetime) we did not attempt to determine the relative triplet yields

(31) (a) Turro, N. J. *Modern Molecular Photochemistry*; Benjamin/Cummings: Menlo Park, CA, 1978; pp 176-180. (b) We cannot directly compare the SPC and picosecond data with these calculated electron-transfer rate constants as the rate constants were determined assuming a single conformation. Both SPC and picosecond data show that this assumption is not true so the utility of eq 1 must be regarded as qualitative.

(32) Darwent, J. R.; Douglas, P.; Harriman, A.; Porter, G.; Richoux, M.-C. *Coord. Chem. Rev.* **1982**, *44*, 83-126.

(33) Felton, R. H. In *The Porphyrins*; Dolphin, D., Ed.; Academic: New York, 1978; Vol. 5.

**TABLE II: Triplet Decay Kinetics of ZnPB<sub>n</sub>R in *p*-Xylene/1-Pentanol (*x/n-p*) and Pyridine (py) at 490 nm**

<i>n</i>	solvent	$\tau_1,^a$ ns	$A_1^b$	$\tau_2,^a$ $\mu$ s	$A_2^c$	$\Delta OD_T / \Delta OD_T^0$
1	<i>x/n-p</i>			280	1.00	0.05
4	<i>x/n-p</i>	160	0.67	290	0.33	<i>e</i>
5	<i>x/n-p</i>	140	0.63	270	0.37	<i>e</i>
6	<i>x/n-p</i>	180	0.60	260	0.40	<i>e</i>
7	<i>x/n-p</i>	140	0.30	280	0.70	<i>e</i>
1	py			300	1.00	0.05
4	py	110	0.10	310	0.90	0.15
5	py	120	0.14	290	0.86	0.20
6	py	140	0.10	320	0.90	0.24
7	py		0.05	290	0.95	0.34

<sup>a</sup> Assumed deviation of  $\pm 20\%$  based on standard deviation.

<sup>b</sup> Relative amplitude of the short-lived species,  $A_1 = \Delta OD_1 / (\Delta OD_1 + \Delta OD_2)$ . <sup>c</sup> Relative amplitude of the long-lived species,  $A_2 = \Delta OD_2 / (\Delta OD_1 + \Delta OD_2)$ . <sup>d</sup> Relative yield of triplet-state formation, where  $\Delta OD_T = \Delta OD_1 + \Delta OD_2$  and  $\Delta OD_T^0$  are the transient absorbances determined for ZnPB<sub>n</sub>R and ZnPB<sub>n</sub>, respectively, at 490 nm immediately after excitation. <sup>e</sup> For *n* = 4–7, no attempts to determine the relative triplet-state yields in *x/n-p* were carried out.

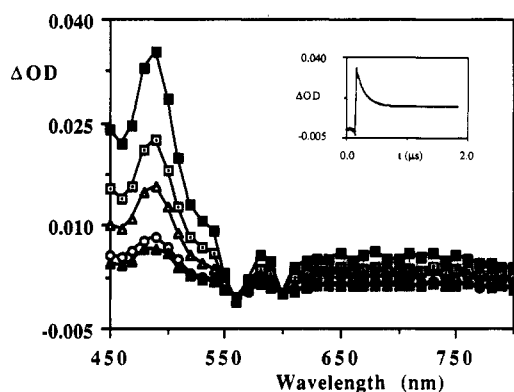


**Figure 6.** Triplet absorption spectra obtained for ZnPB<sub>5</sub>R in *p*-xylene/1-pentanol (■) 0.01  $\mu$ s, (□) 0.07  $\mu$ s, (△) 0.17  $\mu$ s, (○) 0.55  $\mu$ s, and (▲) 1  $\mu$ s after excitation at 532 nm. Inset: decay of the short-lived species at 490 nm.

of ZnPB<sub>n</sub>R in *p*-xylene/1-pentanol and in the microemulsions more accurately (relative triplet yields are measured in pyridine where the amount of fast decaying triplet is considerably decreased, see triplet decay kinetics in pyridine (Table II)).

**B. Triplet Lifetime.** Interestingly, for *n* = 4–7 in *p*-xylene/1-pentanol and in both anionic and cationic microemulsions, two decaying (via first-order kinetics) species with considerably different lifetimes of ca. 160 ns and 280  $\mu$ s are observed, independent of detection wavelength (Table II). The lifetime of the slower component ( $\tau_2$ ) is similar to the triplet-state lifetime of ZnPB<sub>n</sub>.<sup>23</sup> The transient spectra of both decaying species (Figure 6, spectrum after 0.01  $\mu$ s and after 0.55  $\mu$ s) are virtually identical and resemble the triplet spectrum of the uncomplexed porphyrin.<sup>17</sup> A representative decay profile of the fast component is shown in the inset of Figure 6. Again, the existence of ground-state intermolecular dimers can be ruled out as a possible explanation for the observation of two distinct triplet lifetimes since the absorption spectra of the ZnPB<sub>n</sub>R molecules remain unchanged over a wide concentration range.

Interestingly, the length of the bridging chain does not affect the lifetime of either species (Table II) but rather the relative amplitudes of the short-lived component ( $A_1 = \Delta OD_1 / (\Delta OD_1 + \Delta OD_2)$ , where  $\Delta OD$  is the transient absorbance at 490 nm immediately after the laser pulse) and the long-lived component ( $A_2 = \Delta OD_2 / (\Delta OD_1 + \Delta OD_2)$ ) are influenced by the spacer length. For *n* = 4–6, similar relative amplitudes for the short- and the long-lived species are observed, whereas for *n* = 7, the contribution from short-lived species is noticeably reduced, which is consistent with the chain length dependent Soret broadening of MPB<sub>n</sub>R (Table I). For ZnPB<sub>n</sub>R (*n* = 1), only the long-lived component is observed.<sup>17</sup>

The observation of two distinct triplet-state lifetimes in ZnPB<sub>n</sub>R is similarly ascribed to conformational heterogeneity within the RuO<sub>2</sub>-coordinated clusters, consistent with their absorption and fluorescence properties. The faster triplet decay ( $\tau_1$ ) is interpreted as arising from complexed conformers in which electronic interaction between the RuO<sub>2</sub> moiety and the porphyrin  $\pi$ -system appears to reduce the porphyrin triplet-state lifetime. The slower component ( $\tau_2$ ) is assigned to the unperturbed (noncomplexed) porphyrin triplet state. The observation of two distinct porphyrin triplet-state lifetimes ( $\tau_1, \tau_2$ ) suggests that interconversion of the two conformers is slow compared to the triplet-state lifetime.<sup>14</sup> However, the transformation of the short-lived into the long-lived triplet cannot be excluded.

Spectral evidence for two distinct triplet states has also been recently reported for a series of *meso*-tetraalkylporphyrins covalently linked to methyl-*p*-benzoquinone, the corresponding hydroquinone, and dimethoxybenzene.<sup>14</sup> In these molecules, the lifetimes of the two distinct triplet states differ by a factor of ca. 3,<sup>14</sup> whereas in MPB<sub>n</sub>R the triplet-state lifetimes differ by more than 3 orders of magnitude. In MPB<sub>n</sub>R, the strong diminution of the porphyrin triplet-state lifetime in the folded conformers is best explained by enhanced intersystem crossing caused by the heavy atom effect of ruthenium.<sup>34</sup> Spin-orbit coupling may also account for the substantial fluorescence quenching in the perturbed conformers.<sup>34,35</sup>

**Photophysical Studies of MPB<sub>n</sub>R (M = Zn, 2 H) in Pyridine: Blocking of Conformational Folding by Solvent Ligation.** Intramolecular complexation between the porphyrin and the RuO<sub>2</sub> moiety in ZnPB<sub>n</sub>R makes it difficult to distinguish between fluorescence quenching caused by intramolecular electron transfer and enhanced radiationless decay of the porphyrin excited singlet state. (Presumably, the latter process can be attributed to heavy-atom-induced intersystem crossing rather than to internal conversion.<sup>34,35</sup>) For cofacial zinc porphyrin dimers, axial ligation of zinc to pyridine has been found to cause deaggregation of the porphyrins and, thus, a reduction of both exciton coupling (seen in the width of the Soret band) and fluorescence quenching.<sup>36</sup> Deaggregation of the metalloporphyrins by ligand coordination was mainly attributed to a steric effect, i.e., to the blocking of the porphyrin face by pyridine, preventing any  $\pi$ - $\pi$  interaction.<sup>36a</sup> Binding of a donor molecule to a vacant coordination site of a zinc tetraphenylporphyrin (ZnTPP) is known to affect its ground-state absorption<sup>37–39</sup> and fluorescence<sup>40</sup> spectra and its redox properties,<sup>41</sup> but neither the fluorescence quantum yield<sup>40</sup> nor fluorescence lifetime<sup>40</sup> of ZnTPP is changed considerably (within  $\pm 10\%$ , i.e., approximately experimental error). Nor does pyridine quench the triplet state of ZnTPP.<sup>42</sup> Thus, in order to determine the operative decay pathway of the porphyrin excited singlet state, we have examined the photophysical properties (absorption and fluorescence spectra and triplet decay kinetics) of ZnPB<sub>n</sub>R in pyridine where the complexation between the porphyrin and the RuO<sub>2</sub> moiety might be reduced.

Unlike zinc porphyrins, free base porphyrins do not coordinate to pyridine.<sup>38a</sup> Thus, in contrast to ZnPB<sub>n</sub>R, neither absorption

(34) (a) Harriman, A. *J. Chem. Soc., Faraday Trans. 2* **1981**, *77*, 1281–1291. (b) Brookfield, R. L.; Ellul, H.; Harriman, A. *J. Chem. Soc., Faraday Trans. 2* **1985**, *81*, 1837–1848.

(35) Rodriguez, J.; Kirmaier, C.; Holten, D. *J. Am. Chem. Soc.* **1989**, *111*, 6500–6506.

(36) (a) Hunter, C. A.; Leighton, P.; Sanders, J. K. M. *J. Chem. Soc., Perkin Trans. 1* **1989**, 547–552. (b) Hunter, C. A.; Sanders, J. K. M. *J. Am. Chem. Soc.* **1990**, *112*, 5525–5534.

(37) Nappa, M.; Valentine, J. S. *J. Am. Chem. Soc.* **1978**, *100*, 5075–5080.

(38) (a) Miller, J. R.; Dorough, G. D. *J. Am. Chem. Soc.* **1952**, *74*, 3977–3981. (b) Becker, D. S.; Hayes, R. G. *Inorg. Chem.* **1983**, *22*, 3050–3053.

(39) (a) Kirksey, C. H.; Hambricht, P.; Storm, C. B. *Inorg. Chem.* **1969**, *8*, 2141–2144. (b) Kirksey, C. H.; Hambricht, P. *Inorg. Chem.* **1969**, *9*, 958–960. (c) Vogel, G. C.; Beckmann, B. A. *Inorg. Chem.* **1976**, *15*, 483–484.

(40) Humphry-Baker, R.; Kalyanasundaram, K. *J. Photochem.* **1985**, *31*, 105–112.

(41) Kadish, K. M.; Shiue, L. R.; Rhodes, R. K.; Bottomley, L. A. *Inorg. Chem.* **1981**, *20*, 1274–1277.

(42) Pekkarinen, L.; Linschitz, H. *J. Am. Chem. Soc.* **1960**, *82*, 2407–2411.

TABLE III: Soret Bandwidth (fwhm), Relative Fluorescence Quantum Yields, and Calculated Intramolecular Electron-Transfer Rate Constants ( $k_{et}$ ) for ZnPB<sub>n</sub>R and H<sub>2</sub>PB<sub>n</sub>R in Pyridine

M	<i>n</i>	fwhm, <sup>a</sup> nm	$\Phi_f/\Phi_f^0$ <sup>b</sup>	$k_{et}$ <sup>c</sup> × 10 <sup>-9</sup> , s <sup>-1</sup>
Zn	1	11	0.04	17
Zn	4	12	0.16	4.0
Zn	5	12	0.20	3.1
2H	5	17	0.10	0.88
Zn	6	11	0.25	2.3
Zn	7	11	0.32	1.6

<sup>a</sup> Full width at half-height of the absorption maximum of the Soret band. <sup>b</sup> Fluorescence quantum yield of RuO<sub>2</sub>-coordinated MPB<sub>n</sub>( $\Phi_f$ ) relative to the fluorescence quantum yield of uncomplexed MPB<sub>n</sub>( $\Phi_f^0$ ). <sup>c</sup>  $k_{et}$  was calculated from eq 1, assuming a single conformation.

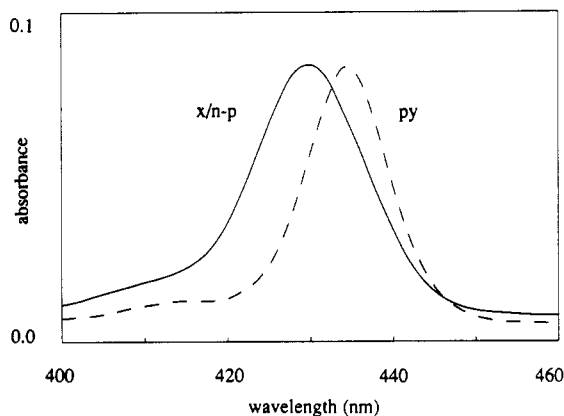


Figure 7. Absorption spectra (Soret region) of ZnPB<sub>3</sub>R in *p*-xylene/1-pentanol (—) and pyridine (---).

nor fluorescence of H<sub>2</sub>PB<sub>n</sub>R is expected to change in pyridine. Studies of the photophysical properties of H<sub>2</sub>PB<sub>n</sub>R in pyridine may thus provide a way to distinguish between spectral changes caused by pyridine ligation or merely by dielectric solvent effects.

**A. Absorption Spectra of ZnPB<sub>n</sub>R and H<sub>2</sub>PB<sub>n</sub>R in Pyridine.** The Soret band and the Q bands of both ZnPB<sub>n</sub>R and ZnPB<sub>n</sub>R are significantly red-shifted in pyridine (434, 568, and 608 nm) compared to their positions in *p*-xylene/1-pentanol (430, 560, and 602 nm) and in THF (427, 558, and 600 nm), and the intensity of the Q<sub>(0,0)</sub> band relative to the Q<sub>(1,0)</sub> band is increased. However, in pyridine, the Soret bands of ZnPB<sub>n</sub>R (fwhm = 11 nm, Table III) are not broader than those of ZnPB<sub>n</sub>R (fwhm = 11 nm), whereas the absorption spectra of ZnPB<sub>n</sub>R in THF and *p*-xylene/1-pentanol, and in the microemulsions show broadened Soret bands (Table I) (Figure 7). If the broadening of the Soret band implies intramolecular complexation between the  $\pi$ -electron system of the porphyrin and the RuO<sub>2</sub> cluster, the absence of such spectral broadening in pyridine suggests a reduction of this complexation. Thus, the strong axial ligation of the zinc porphyrin to pyridine<sup>38a</sup> influences the distributions of conformers in the linked molecules so as to prevent the RuO<sub>2</sub> moiety from reaching over the porphyrin  $\pi$ -system by folding of the flexible alkyl chain.<sup>43</sup>

For the free base derivative, H<sub>2</sub>PB<sub>n</sub>R, where no pyridine ligation occurs, similar absorption spectra are observed in pyridine and *p*-xylene/1-pentanol, i.e., the Soret bandwidth of H<sub>2</sub>PB<sub>3</sub>R does not change in pyridine (fwhm = 17 nm, Table III) compared to other solvents (fwhm = 17 nm both in THF and *p*-xylene/1-pentanol, Table I).

**B. Fluorescence Spectra and Relative Fluorescence Quantum Yields of ZnPB<sub>n</sub>R and H<sub>2</sub>PB<sub>n</sub>R in Pyridine.** The fluorescence spectrum of ZnPB<sub>3</sub>R is red-shifted in pyridine (619 and 669 nm) compared to that in *p*-xylene/1-pentanol (610 and 660 nm) (Figure 8) and similar shifts are also observed with other ZnPB<sub>n</sub>R and ZnPB<sub>n</sub>R. As expected, for ZnPB<sub>n</sub>R (*n* = 4–7), fluorescence quenching in pyridine (Table III) is less efficient than that in *p*-xylene/1-pentanol (x/n-p)<sup>44</sup> and THF (Table I) (Figure 8) since

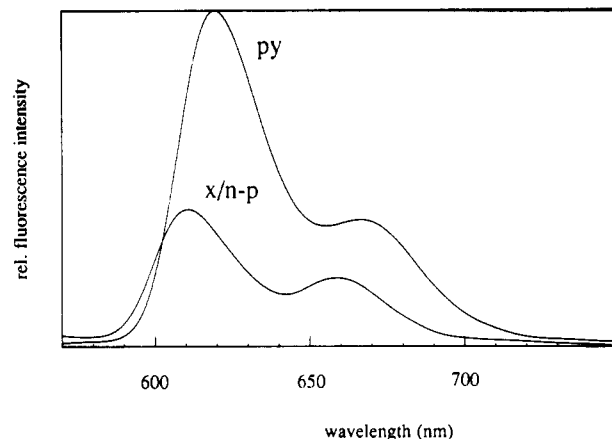


Figure 8. Uncorrected fluorescence spectra of ZnPB<sub>3</sub>R in *p*-xylene/1-pentanol (x/n-p) and pyridine (py). Excitation was at 430 nm (x/n-p) and at 434 nm (py).

pyridine blocks the complexed conformation in which quenching occurs. This reduced fluorescence quenching in pyridine may also conceivably be caused by a change in the redox potentials of the zinc porphyrin<sup>41</sup> and/or the RuO<sub>2</sub> particles with solvent. In pyridine, the surface of the RuO<sub>2</sub> cluster could also change: for example, surface adsorption of solvent at acidic sites may occur. However, changes in the cluster character (redox potentials or surface) in pyridine cannot explain the absence of a broadening of the porphyrin Soret band in this solvent. The observed increase in relative fluorescence quantum yield of ZnPB<sub>n</sub>R in pyridine is, however, consistent with our assumption that, in the complexed conformers, the porphyrin fluorescence is substantially quenched.

The increase in relative fluorescence quantum yield of ZnPB<sub>n</sub>R in pyridine (Table III) compared to *p*-xylene/1-pentanol<sup>44</sup> and THF (Table I) and thus the contribution of complexed conformers clearly depends on the spacer length, *n*. For *n* = 1 (pyridine  $\Phi_f/\Phi_f^0$  = 0.04; THF<sup>44</sup>  $\Phi_f/\Phi_f^0$  = 0.03), where intramolecular complexation is expected to be negligible, the relative fluorescence quantum yield is almost solvent independent. Complexation is apparently optimal for *n* = 4 (0.16 and 0.06, respectively, in pyridine and THF) and 5 (0.20 and 0.09, respectively), whereas for *n* = 7 (0.32 and 0.27, respectively) complexation seems to be more or less hindered by chain length.

In contrast to ZnPB<sub>n</sub>R, H<sub>2</sub>PB<sub>n</sub>R show similar fluorescence spectra and the same fluorescence quenching in pyridine (Table III) and *p*-xylene/1-pentanol (which is similar to that in THF, Table I). The fact that both the Soret bandwidth and the relative fluorescence quantum yield of H<sub>2</sub>PB<sub>n</sub>R are unaffected by pyridine suggests that the absence of spectral broadening and the increased relative fluorescence quantum yields of ZnPB<sub>n</sub>R in pyridine are clearly caused by axial ligation of pyridine to the zinc porphyrin rather than dielectric effects.

**C. Effect of Pyridine Coordination on Triplet Decay Kinetics of ZnPB<sub>n</sub>R.** For ZnPB<sub>n</sub>R in pyridine, a transient with a spectrum identical with that in Figure 6 is observed, which like the triplet in *p*-xylene/1-pentanol, exhibits two decay lifetimes of ca. 130 ns and 300  $\mu$ s (Table II). However, in pyridine, substantially smaller contributions from the short-lived component ( $\tau_1$ ) than in *p*-xylene/1-pentanol can be seen (Table II), suggesting minimal complexation between the porphyrin and RuO<sub>2</sub> in pyridine, consistent with the absorption and fluorescence studies.

The substantially smaller amounts of short-lived triplet in pyridine enabled us to determine the triplet yield of ZnPB<sub>n</sub>R relative to those of ZnPB<sub>n</sub>R. For ZnPB<sub>n</sub>R, the relative triplet yields ( $\Delta OD_T/\Delta OD_T^0$ , where  $\Delta OD_T$  and  $\Delta OD_T^0$  are the transient absorbances determined for ZnPB<sub>n</sub>R and ZnPB<sub>n</sub>R, respectively, at 490 nm immediately after excitation) (Table II) are reduced to a similar extent as the relative fluorescence quantum yields (Table III).

(43) Boxer, S. G.; Bucks, R. R. *J. Am. Chem. Soc.* 1979, 101, 1883–1885.

(44) For ZnPB<sub>n</sub>R, the same relative fluorescence quantum yields were obtained both in THF and *p*-xylene/1-pentanol.

TABLE IV: Fluorescence Lifetimes of ZnPB<sub>n</sub>R in *p*-Xylene/1-Pentanol (x/n-p) and Pyridine (py) Determined by SPC

sample	solvent	$\tau_1$ , <sup>a</sup> ns	$A_1$ <sup>b</sup>	$\tau_2$ , <sup>a</sup> ns	$A_2$	$\tau_3$ , <sup>a</sup> ns	$A_3$	$\chi^2$
ZnP	x/n-p					1.43	1.00	1.22
ZnP	py					1.40	1.00	1.13
ZnPB <sub>3</sub>	x/n-p					1.44	1.00	1.31
ZnPB <sub>3</sub>	py					1.42	1.00	1.20
ZnPB <sub>4</sub> R	x/n-p	0.028	0.88	0.17	0.10	1.22	0.02	1.06
ZnPB <sub>4</sub> R	py	0.031	0.77	0.16	0.10	1.41	0.14	1.12
ZnPB <sub>5</sub> R	x/n-p	0.044	0.82	0.32	0.14	1.23	0.06	1.14
ZnPB <sub>5</sub> R	py	0.041	0.77	0.32	0.14	1.29	0.09	0.98
ZnPB <sub>6</sub> R	x/n-p	0.053	0.78	0.37	0.14	1.22	0.08	1.22
ZnPB <sub>6</sub> R	py	0.051	0.75	0.35	0.15	1.30	0.10	1.05
ZnPB <sub>7</sub> R	x/n-p	0.072	0.67	0.42	0.19	1.19	0.14	1.06
ZnPB <sub>7</sub> R	py	0.068	0.68	0.42	0.18	1.28	0.14	0.98
ZnPB <sub>7</sub> R	x/n-p	0.093	0.57	0.56	0.23	1.31	0.20	1.07
ZnPB <sub>7</sub> R	py	0.089	0.59	0.55	0.21	1.30	0.20	1.06

<sup>a</sup>An average deviation of  $\pm 5\%$  was observed for each fluorescence lifetime. <sup>b</sup>Relative amplitude (fit parameter) of the component with the fluorescence lifetime  $\tau_1$ . <sup>c</sup>ZnPB<sub>4</sub>R to which ca. 10% ZnP was added.

Studies of the absorption and fluorescence properties as well as the triplet decay kinetics of ZnPB<sub>n</sub>R in pyridine, *p*-xylene/1-pentanol, and THF show that the increase in the relative fluorescence quantum yield for ZnPB<sub>n</sub>R in pyridine (Table III), the extent of broadening of the Soret bands in THF or *p*-xylene/1-pentanol (Table I), and the relative amplitude of short-lived triplet in *p*-xylene/1-pentanol (Table II) depend similarly on the spacer length, *n*, with all effects being more pronounced for *n* = 4–6 than for *n* = 7. This suggests a higher fraction of the complexed conformers for *n* = 4–6 than for *n* = 7. The fact that, for ZnPB<sub>4</sub>R (*n* = 1), the extent of fluorescence quenching is more or less unaffected by pyridine and only one triplet lifetime is observed suggests that for *n* = 1, presumably no folding occurs. However, in pyridine, where intramolecular complexation between the porphyrin  $\pi$ -system and the RuO<sub>2</sub> particles in MPB<sub>n</sub>R has been shown to be minimal, both the porphyrin fluorescence intensities (Table III) and triplet yields (Table II) of ZnPB<sub>n</sub>R are also substantially reduced relative to those of ZnPB<sub>n</sub>. Thus, the efficient fluorescence quenching in MPB<sub>n</sub>R cannot be merely explained by complexation of the two chromophores. Instead, we suggest that an additional route, probably electron transfer from the porphyrin excited singlet state to the RuO<sub>2</sub> cluster, must also contribute to the observed fluorescence quenching.

**Dependence of Fluorescence Lifetimes of ZnPB<sub>n</sub>R on Spacer Chain Length in *p*-Xylene/1-Pentanol and Pyridine.** The lifetimes of the first excited singlet states of ZnP, ZnPB<sub>n</sub>, and ZnPB<sub>n</sub>R were measured by time-correlated single photon counting in both dilute *p*-xylene/1-pentanol (x/n-p) where intramolecular complexation between the porphyrin and the RuO<sub>2</sub> cluster occurs and in pyridine (py) where this complexation is minimal (Table IV). A comparison between the fluorescence lifetimes in both solvents thus allows us to determine the contributions from the complexed conformers to the fluorescence decay kinetics.

Fluorescence intensity decay profiles of ZnP (which is virtually identical with those of ZnPB<sub>n</sub>) and ZnPB<sub>n</sub>R in *p*-xylene/1-pentanol (Figure 9) show that the singlet-state lifetimes of ZnPB<sub>n</sub>R are considerably shorter than those of the uncomplexed porphyrin. The fluorescence profiles of ZnP and ZnPB<sub>n</sub> could be analyzed satisfactorily by single-exponential fits ( $\chi^2 = 1.1$ –1.3). The three-exponential fit<sup>45</sup> of the fluorescence decay profiles of ZnPB<sub>n</sub>R in *p*-xylene/1-pentanol and pyridine gave lifetimes of 0.03–0.09 ns ( $\tau_1$ ), 0.15–0.56 ns ( $\tau_2$ ), and 1.2–1.3 ns ( $\tau_3$ ) with relative amplitudes of 0.6–0.9 ( $A_1$ ), 0.1–0.2 ( $A_2$ ), and 0.02–0.20 ( $A_3$ ) and  $\chi^2$  values of 1.0–1.1 (Table IV).

The fluorescence lifetimes and relative amplitudes (kinetic fit parameters) of ZnPB<sub>n</sub>R in *p*-xylene/1-pentanol and pyridine are very similar, indicating that, for the fluorescence lifetime mea-

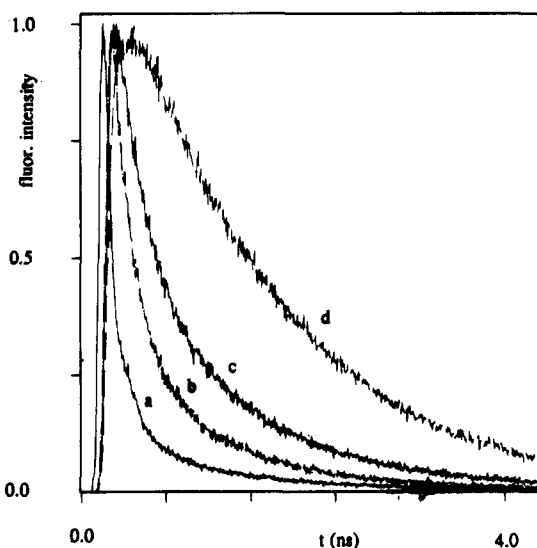


Figure 9. Fluorescence intensity decay profiles of (a) ZnPB<sub>4</sub>R, (b) ZnPB<sub>5</sub>R, (c) ZnPB<sub>6</sub>R, and (d) ZnP recorded by the single photon counting technique in *p*-xylene/1-pentanol. After deconvolution of the instrumental response function, the decay profiles of ZnPB<sub>n</sub>R were analyzed as the sum of both two- and three-exponential terms.

surements, no contributions from the complexed conformers are observed. This suggests complete fluorescence quenching in the complexed conformers (whose relative distribution as a function of chain length is clear from the discussion above and the relative quantum yields described in Tables I and III). Thus, the multiexponential fluorescence kinetics derive entirely from the non-complexed fluorescent conformers.

The complete fluorescence quenching in the complexed conformers may be attributed to very fast intersystem crossing, thus allowing for observation of a complexed triplet (see Table II) under conditions in which the complexed singlet is completely quenched. In contrast, as we should see below, electron transfer is likely the major decay route for the noncomplexed conformers.

For ZnPB<sub>n</sub>R in both solvents, triplet-exponential fits result in two fast processes with lifetimes of 0.03–0.09 ns ( $\tau_1$ ) and 0.15–0.56 ns ( $\tau_2$ ) dependent on chain length and a much slower process with a lifetime of ca. 1.2 ns, independent of chain length (Table IV). For all ZnPB<sub>n</sub>R molecules, the fluorescence decay profiles are dominated by the shortest lived component. The relative amplitudes depend on the length of the bridging chain: the relative amount of the (dominant) shortest lived species ( $A_1$ ) decreases with increasing chain length (Table IV). The longest lived species ( $\tau_3$ ) has a lifetime comparable to that of the unbound porphyrin ZnP: the possibility that it is an impurity (ZnP or uncomplexed ZnPB<sub>n</sub>) is rather unlikely, since we place the maximum impurity level at  $\ll 5\%$  (TLC), which cannot account for the relative amplitudes ( $A_3$ ) seen in the longest lived species, especially for *n* = 6, 7. Furthermore, a control experiment carried out with ZnPB<sub>4</sub>R

(45) The fluorescence decay profiles of ZnPB<sub>n</sub>R were fit to the sum of two exponentials resulting in lifetimes of 0.06–0.19 ns ( $\tau_1$ ) and 1.0–1.2 ns ( $\tau_3$ ) with relative amplitudes of 0.70–0.95 ( $A_1$ ) and 0.05–0.30 ( $A_3$ ). The high  $\chi^2$  values indicate multiexponential behavior ZnPB<sub>n</sub>R: thus, a three-exponential analysis was performed for these compounds. However, the three-exponential fits of the fluorescence profiles may represent a more complex distribution.

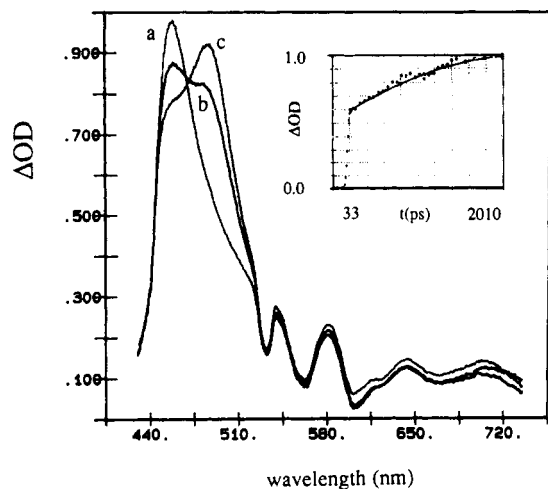


**Figure 10.** Transient absorption difference spectra recorded various times after excitation ( $\lambda = 532$  nm) of ZnP in *p*-xylene/1-pentanol with a 30-ps laser pulse: (a) immediately after excitation; (b) 1056 ps and (c) 2112 ps after excitation. Transient absorption profiles were recorded at 465 and 490 nm (inset) and analyzed by first-order kinetics, giving  $k_{\text{obs}}^0$  of  $(9 \pm 3) \times 10^8 \text{ s}^{-1}$ .

to which ca. 10% ZnP was added shows that, in the presence of added porphyrin, the lifetime of the longest lived species is equivalent to the lifetime of ZnP, i.e., longer than  $\tau_3$ .

Fluorescence decays of flexible donor-acceptor systems are often interpreted as contributions of at least two different sets of conformations: folded conformations with closely spaced donor and acceptor in which fluorescence quenching is efficient and extended forms which show little energy or electron transfer because of either the large separation distance or unfavorable orientation factors.<sup>14,46</sup> Thus, the triple-exponential fluorescence decay of ZnPB<sub>n</sub>R suggests the existence of more than one family of non-complexed fluorescent conformers with varying separation distance or orientation between the porphyrin and the RuO<sub>2</sub> cluster. Furthermore, the fluorescence decay kinetics in ZnPB<sub>n</sub>R may be complicated by the size distribution of the attached RuO<sub>2</sub> cluster, which in turn could affect the cluster's effective redox potential.

**Characterization of Singlet Decay Kinetics of ZnPB<sub>n</sub>R by Picosecond Absorption Spectroscopy.** The decay kinetics of the porphyrin excited singlet states of ZnP and ZnPB<sub>n</sub>R were studied in *p*-xylene/1-pentanol and in both microemulsions with subnanosecond time-resolved absorption spectroscopy in order to determine the decay pathway of the porphyrin excited singlet in ZnPB<sub>n</sub>R, i.e., whether the porphyrin radical cation is formed and whether ultrafast intersystem crossing occurs. The singlet decay kinetics were found to be independent of solvent.

**A. Singlet Decay Kinetics of ZnP.** Picosecond flash photolysis of ZnP reveals immediate formation of a transient absorption band with a sharp maximum at 465 nm (Figure 10) which is assigned to the porphyrin excited singlet state ( $S_1 \rightarrow S_n$  transition) and which slowly decreases as a new band at 490 nm grows in concomitantly (spectra b and c). The absorption band at 490 nm is assigned to the porphyrin triplet state ( $T_1 \rightarrow T_n$  transition) (Figure 6). Both from the decrease of the absorbance at 465 nm and the increase at 490 nm a rate constant  $k_{\text{obs}}^0$  was determined to  $(9 \pm 3) \times 10^8 \text{ s}^{-1}$  with  $k_{\text{obs}}^0 = k_f^0 + k_{\text{isc}}^0 + k_{\text{ic}}^0$  ( $k_f^0$ , radiative rate constant;  $k_{\text{isc}}^0$ , rate constant for intersystem crossing; and  $k_{\text{ic}}^0$ , rate constant for internal conversion).

For metalloporphyrins,<sup>47</sup> both the rate constant for intersystem crossing ( $k_{\text{isc}}^0$ ) and the rate of radiative decay from the porphyrin excited singlet state ( $k_f^0$ ) can be calculated from the fluorescence

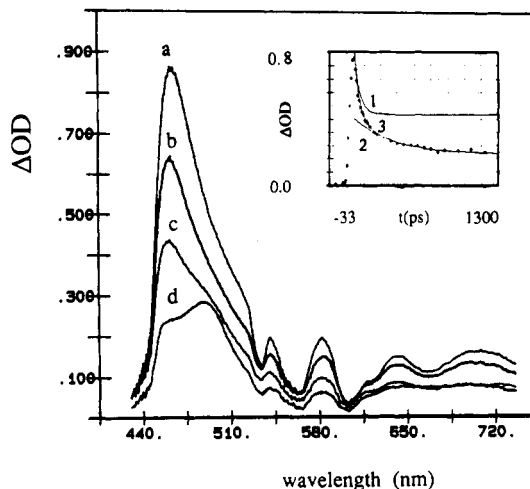


**Figure 11.** Transient absorption difference spectra recorded various times after excitation ( $\lambda = 532$  nm) of ZnPB<sub>5</sub>R in *p*-xylene/1-pentanol with a 30-ps laser pulse: (a) immediately after excitation; (b) 145 ps, (c) 343 ps, and (d) 1465 ps after excitation. The absorbance decay profile at 465 nm is shown in the inset. The decay profile was analyzed as the sum of two first-order processes, giving lifetimes of (1) 53 ps and (2) 380 ps. Trace 3 shows the actual decay profile and the computed fit.

quantum yield ( $\Phi_f^0$ ) and the observed (experimental) fluorescence lifetime ( $\tau_f^0$ ), assuming that the sum of the quantum yields of fluorescence ( $\Phi_f^0$ ) and intersystem crossing ( $\Phi_{\text{isc}}^0$ ) is close to unity and, thus  $k_{\text{isc}}^0 \gg k_{\text{ic}}^0$ :

$$k_{\text{isc}}^0 = k_f^0(1 - \Phi_f^0)/\Phi_f^0 \quad (2)$$

$$k_f^0 = \Phi_f^0/\tau_f^0 \quad (3)$$

For ZnTPP and its *p*-ethoxyphenyl derivative, fluorescence quantum yields of 0.03 and 0.033 have been reported in benzene.<sup>47</sup> Assuming that  $\Phi_f^0(\text{ZnP})$  equals  $\Phi_f^0(\text{ZnTPP})$ ,  $k_f^0$  was calculated as  $2.1 \times 10^7 \text{ s}^{-1}$  and  $k_{\text{isc}}^0$  as  $6.9 \times 10^8 \text{ s}^{-1}$ , which is in good agreement with  $k_{\text{obs}}^0$  determined by picosecond flash photolysis.

**B. Singlet Decay Kinetics of ZnPB<sub>n</sub>R.** For ZnPB<sub>5</sub>R, the porphyrin excited singlet state is also formed immediately after excitation (Figure 11, spectrum a). The absorption at 465 nm decreases by approximately 50% during the first 350 ps following the excitation pulse (spectra b and c), but the absorption profile which shows a weak shoulder at 490 nm (where the triplet absorbs) does not change considerably. A further decrease in absorbance occurs over the next 1.1 ns, revealing an absorbance at 490 nm (spectrum d) which is attributed to the porphyrin triplet state. The decay profile of the porphyrin excited singlet at 465 nm (inset of Figure 11) was analyzed in terms of two competing first-order processes with lifetimes of (a) 55 ps and (b) 380 ps. The singlet-state lifetimes determined by picosecond absorption spectroscopy of ZnPB<sub>n</sub>R are in good agreement with the fluorescence lifetimes ( $\tau_1$  and  $\tau_2$ ) determined by SPC (Table IV).<sup>48</sup>

A comparison of the ratios of the absorbances at 465 nm (singlet) and 490 nm (triplet) for ZnP (Figure 10, spectrum c) and ZnPB<sub>5</sub>R (Figure 11, spectra a and d) indicates (1) that no considerable amount of porphyrin triplet is formed immediately after excitation of ZnPB<sub>5</sub>R (Figure 11, spectrum a) and (2) a considerably lower triplet yield for ZnPB<sub>5</sub>R (Figure 11, spectrum d). This suggests electron transfer rather than enhanced intersystem crossing as a major decay route of the excited singlet in ZnPB<sub>5</sub>R.<sup>35</sup>

The complex singlet decay kinetics of ZnPB<sub>n</sub>R may be best explained by electron-transfer reactions occurring in different sets of noncomplexed conformations which do not equilibrate on a subnanosecond time scale.<sup>9e</sup> The very short singlet-state lifetimes suggest electron transfer between proximal partners within a family

(46) Brookfield, R. L.; Ellul, H.; Harriman, A.; Porter, G. *J. Chem. Soc., Faraday Trans. 2* **1986**, *82*, 219-233.

(47) (a) Ohno, O.; Kaizu, Y.; Kobayashi, H. *J. Chem. Phys.* **1985**, *82*, 1779-1787. (b) Hurley, J. K.; Sinai, N.; Linschitz, H. *Photochem. Photobiol.* **1983**, *38*, 9-14. Although the precise value of  $\Phi_T$  ( $\Phi_{\text{isc}}$ ) and  $\Phi_f$  is controversial (for ZnTPP, the reported  $\Phi_T$  is  $0.83 \pm 0.04$ ),<sup>47b</sup> this value is close enough to unity for this qualitative analysis to still be pertinent.

(48) The singlet decay profiles were fit to the sum of two exponentials rather than to three exponentials, i.e., neglecting the longest lived components ( $\tau_3$ ) shown in Table IV. The growth of the triplet is presumably the longest lived singlet component (both in absorption and emission).

of conformations. Small molecular separation favors rapid forward electron transfer, but unless the products can migrate apart quickly, rapid back electron transfer follows.<sup>13,49</sup> Very rapid back electron transfer might explain our inability to observe the radical cation, even for the longer chain length systems.<sup>9,10</sup> The slower process could be associated with a group of conformations in which the RuO<sub>2</sub> cluster is held at some distance away from the porphyrin. This hypothesis assumes that electron transfer occurs by direct interaction between the porphyrin and RuO<sub>2</sub> in these close (noncomplexed) conformers (through space) rather than through the connecting bridge. Partial support for this hypothesis may arise from the relatively small changes in the singlet-state lifetimes of ZnPB<sub>*n*</sub>R upon varying *n*.<sup>7,9,10b</sup>

### Conclusions

The broadening of the porphyrin Soret band and the observation of two distinct triplet-state lifetimes in MPB<sub>*n*</sub>R are best interpreted as arising from at least two distinct families of conformers: (1) complexed conformers in which folding of the RuO<sub>2</sub> moiety over the porphyrin  $\pi$ -system results in intramolecular complexation between the two chromophores and (2) one or more extended (noncomplexed) conformers. The complexed conformers, which are most likely nonfluorescent, exhibit broadened absorption spectra and strongly reduced triplet-state lifetimes compared to the noncomplexed conformers. In the complexed conformers, electronic interaction between the porphyrin and the RuO<sub>2</sub> cluster via spin-orbit coupling leads to a substantial decrease of the porphyrin triplet-state lifetime. The observation of two distinct porphyrin triplet-state lifetimes suggests that interconversion of the two conformers is slow compared to the triplet lifetime. Absorption and fluorescence properties, as well as triplet decay kinetics, indicate that the distributions of the conformers depends on the length of the flexible linkage: the fraction of complexed conformers seems to be higher for *n* = 4–6 than for *n* = 7. For *n* = 1, presumably no folding occurs.

Coordination to pyridine at the axial site of the zinc porphyrin of ZnPB<sub>*n*</sub>R leads to a reduction of the contribution of complexed conformers as indicated by unperturbed absorption spectra, increased relative fluorescence quantum yields, and the considerable decrease in the relative amount of fast decaying porphyrin triplet. Axial pyridine ligation of the zinc porphyrin appears to prevent the RuO<sub>2</sub> cluster from folding over the porphyrin  $\pi$ -system, reducing the contributions of complexed conformers. However, even for ZnPB<sub>*n*</sub>R in pyridine, the fluorescence intensity, the triplet yield, and the singlet-state lifetime of the porphyrin are still substantially decreased relative to the unbound porphyrin, whereas the triplet-state lifetime is unaffected, suggesting that another pathway, presumably electron transfer, is the major decay route of the porphyrin excited singlet state in the noncomplexed conformers. In the complexed, nonfluorescent conformers, very fast intersystem crossing rather than electron transfer may be operative. In MPB<sub>*n*</sub>R, electron transfer may occur either by direct interaction between the porphyrin and the RuO<sub>2</sub> in the close (noncomplexed) conformers (through space) or along the linking chain. The relatively small changes in the singlet-state lifetimes of ZnPB<sub>*n*</sub>R with varying *n* may provide support for electron transfer occurring at least partially through space.

**Acknowledgment.** We thank D. J. Kiserow for help with the time-resolved fluorescence measurements, Dr. S. M. Hubig for assistance in the subnanosecond time-resolved absorption measurements, and Drs. B. A. Gregg, Y.-P. Sun, J. Waluk, and V. Balaji for stimulating discussions. Financial support of the work by the Office of Basic Energy Science, U.S. Department of Energy and the Robert A. Welch Foundation is gratefully acknowledged. The Wigner Foundation graciously provided support for U.R. The flash photolysis experiments were performed at the Center for

Fast Kinetics Research, which is supported jointly by the Biomedical Research Technology Program of the Division of Research Resources of the National Institute of Health (RR00886) and by the University of Texas at Austin.

### Appendix: Spectral Data

**4-(4-Bromobutyl)-4'-methyl-2,2'-bipyridine (B<sub>4</sub>).** Yield: 51% of a white solid, mp 53–54 °C. <sup>1</sup>H NMR (ppm):  $\delta$  1.84–1.91 (m, 4 H),  $\delta$  2.41 (s, 3 H),  $\delta$  2.71 (t (*J* = 7.5 Hz), 2 H),  $\delta$  3.40 (t (*J* = 6.5 Hz), 2 H),  $\delta$  7.11–7.12 (m, 2 H),  $\delta$  8.21 (m, 2 H),  $\delta$  8.51–8.55 (m, 2 H). <sup>13</sup>C NMR (ppm):  $\delta$  21.1, 28.7, 32.1, 33.2, 34.5, 121.2, 122.0, 123.7, 124.7, 148.1, 148.9, 149.0, 151.7, 155.9, 156.2. MS (EI), *m/e*: calcd for C<sub>15</sub>H<sub>17</sub>N<sub>2</sub><sup>79</sup>Br, 304.05751; found 304.05649.

**4-(5-Bromopentyl)-4'-methyl-2,2'-bipyridine (B<sub>5</sub>).** Yield: 41% of a white waxy solid, mp 30–32 °C. <sup>1</sup>H NMR (ppm):  $\delta$  1.48–1.52 (m, 2 H),  $\delta$  1.68–1.73 (m, 2 H),  $\delta$  1.85–1.89 (m, 2 H),  $\delta$  2.41 (s, 3 H),  $\delta$  2.69 (t (*J* = 7.5 Hz), 2 H),  $\delta$  3.38 (t (*J* = 6.5 Hz), 2 H),  $\delta$  7.10–7.11 (m, 2 H),  $\delta$  8.20–8.21 (m, 2 H),  $\delta$  8.50–8.53 (m, 2 H). <sup>13</sup>C NMR (ppm):  $\delta$  21.2, 27.8, 29.5, 32.5, 33.5, 35.3, 121.2, 122.0, 123.8, 124.6, 148.1, 148.9, 149.0, 152.2, 156.0, 156.2. MS (EI), *m/e*: calcd for C<sub>16</sub>H<sub>19</sub>N<sub>2</sub><sup>79</sup>Br, 318.0732; found 318.0732.

**4-(7-Bromoheptyl)-4'-methyl-2,2'-bipyridine (B<sub>7</sub>).** Yield: 47% of a white solid, mp 40–41 °C. <sup>1</sup>H NMR (ppm):  $\delta$  1.31–1.34 (m, 4 H),  $\delta$  1.38–1.41 (m, 2 H),  $\delta$  1.65–1.68 (m, 2 H),  $\delta$  1.78–1.84 (m, 2 H),  $\delta$  2.40 (s, 3 H),  $\delta$  2.65 (t (*J* = 7.5 Hz), 2 H),  $\delta$  3.36 (t (*J* = 6.5 Hz), 2 H),  $\delta$  7.09–7.10 (m, 2 H),  $\delta$  8.18–8.19 (m, 2 H),  $\delta$  8.50–8.52 (m, 2 H). <sup>13</sup>C NMR (ppm):  $\delta$  21.1, 28.0, 28.5, 29.0, 30.2, 32.7, 33.9, 35.4, 121.2, 122.0, 123.9, 124.6, 148.1, 148.9, 148.9, 152.7, 156.0, 156.1. MS (EI), *m/e*: calcd for C<sub>18</sub>H<sub>23</sub>N<sub>2</sub><sup>79</sup>Br, 346.1044; found 346.1034.

**ZnPB<sub>4</sub>.** Yield: 50% of a purple solid, mp 186–189 °C. <sup>1</sup>H NMR (ppm):  $\delta$  0.93 (t (*J* = 7.0 Hz), 9 H),  $\delta$  1.34–1.48 (m, 24 H),  $\delta$  1.59–1.62 (m, 6 H),  $\delta$  1.94–1.97 (m, 10 H),  $\delta$  2.41 (s, 3 H),  $\delta$  2.76 (t (*J* = 7.5 Hz), 2 H),  $\delta$  4.20 (t (*J* = 6.5 Hz), 8 H),  $\delta$  7.17–7.27 (m, 10 H),  $\delta$  8.07–8.09 (m, 8 H),  $\delta$  8.26–8.37 (m, 2 H),  $\delta$  8.56–8.64 (m, 2 H),  $\delta$  8.90–8.91 (m, 8 H). <sup>13</sup>C NMR (ppm):<sup>25</sup>  $\delta$  14.2, 21.2, 22.7, 26.2, 27.0, 29.1, 29.3, 29.5, 31.8, 31.9, 35.2, 67.7, 68.9, 112.5, 112.7, 120.0, 120.8, 121.3, 122.0, 122.7, 123.9, 124.6, 124.7, 131.1, 131.2, 131.2, 135.0, 135.2, 135.3, 135.4, 135.5, 148.7, 148.7, 148.8, 149.0, 149.2, 149.9, 150.5, 158.7. MS (FAB), *m/e*: calcd for C<sub>83</sub>H<sub>92</sub>O<sub>4</sub>N<sub>6</sub>Zn, 1301; found 1301.

**ZnPB<sub>5</sub>.** Yield: 74% of a purple solid, mp 130–133 °C. <sup>1</sup>H NMR (ppm):  $\delta$  0.92 (t (*J* = 7.0 Hz), 9 H),  $\delta$  1.32–1.46 (m, 24 H),  $\delta$  1.57–1.61 (m, 6 H),  $\delta$  1.66–1.68 (m, 2 H),  $\delta$  1.83–1.86 (m, 2 H),  $\delta$  1.93–1.97 (m, 8 H),  $\delta$  2.43 (s, 3 H),  $\delta$  2.72 (t (*J* = 7.5 Hz), 2 H),  $\delta$  4.20 (t (*J* = 6.5 Hz), 8 H),  $\delta$  7.19–7.28 (m, 10 H),  $\delta$  8.06–8.08 (m, 8 H),  $\delta$  8.24–8.36 (m, 2 H),  $\delta$  8.52–8.61 (m, 2 H),  $\delta$  8.90–8.91 (m, 8 H). <sup>13</sup>C NMR (ppm):<sup>25</sup>  $\delta$  13.9, 21.1, 22.4, 25.7, 26.0, 29.1, 29.2, 29.3, 29.4, 30.1, 31.6, 35.3, 67.5, 68.0, 112.00, 119.90, 120.90, 121.6, 122.5, 122.7, 122.9, 123.1, 123.2, 125.2, 131.1, 131.2, 131.2, 135.0, 135.23, 135.4, 135.5, 135.7, 148.5, 148.6, 148.8, 149.0, 149.2, 150.0, 150.0, 158.3. MS (FAB), *m/e*: calcd for C<sub>84</sub>H<sub>94</sub>O<sub>4</sub>N<sub>6</sub>Zn, 1315; found 1315.

**ZnPB<sub>7</sub>.** Yield: 57% of a purple solid, mp 134–137 °C. <sup>1</sup>H NMR (ppm):<sup>24</sup>  $\delta$  0.94 (t (*J* = 7.0 Hz), 9 H),  $\delta$  1.34–1.50 (m, 30 H),  $\delta$  1.58–1.64 (m, 8 H),  $\delta$  1.76–1.79 (m, 2 H),  $\delta$  1.93–1.99 (m, 8 H),  $\delta$  2.40 (s, 3 H),  $\delta$  4.21 (t (*J* = 6.5 Hz), 8 H),  $\delta$  7.16–7.25 (m, 10 H),  $\delta$  8.08–8.10 (m, 8 H),  $\delta$  8.25–8.30 (m, 2 H),  $\delta$  8.47–8.58 (m, 2 H),  $\delta$  8.90–8.91 (m, 8 H). <sup>13</sup>C NMR (ppm):<sup>25</sup>  $\delta$  13.9, 20.9, 22.5, 25.9, 26.0, 29.0, 29.1, 29.3, 29.3, 29.5, 30.2, 31.5, 31.6, 35.3, 67.9, 68.0, 112.0, 119.9, 121.1, 121.8, 122.7, 122.9, 123.1, 123.7, 124.4, 124.4, 131.1, 131.2, 131.3, 135.0, 135.2, 135.2, 135.3, 135.6, 148.7, 148.8, 149.0, 149.00, 149.2, 149.3, 150.1, 158.3. MS (FAB), *m/e*: calcd for C<sub>86</sub>H<sub>98</sub>O<sub>4</sub>N<sub>6</sub>Zn, 1343; found 1343.

**Registry No.** B<sub>4</sub>, 115008-03-2; B<sub>5</sub>, 122397-43-7; B<sub>6</sub>, 134706-74-4; B<sub>7</sub>, 134706-75-5; ZnPB<sub>6</sub>, 134734-92-2; RuO<sub>2</sub>, 12036-10-1.

(49) Harriman, A.; Nowak, A. K. *Pure Appl. Chem.* 1990, 62, 1107–1110.